



## EFFECT OF FOUNDATION SOIL ON DYNAMIC STABILITY OF EMBANKMENT DAMS: NUMERICAL ILLUSTRATIONS UNDERTAKEN USING THE FLAC<sup>3D</sup> AND PLAXIS GEOTECHNICAL SOFTWARES

---

Shiferaw Henok Marie

*Author Details*

*Henok Marie is currently a lecturer at University of Gondar, Civil engineering department, Gondar, Ethiopia, PH+251-935-66-54-53, E-mail: henokmarie@yahoo.com*

**KeyWords:** dynamic stability of embankment, finite difference, finite element, linearly elastic perfectly plastic constitutive model, loose foundation soil, numerical modeling, FLAC<sup>3D</sup>, PLAXIS

### ABSTRACT

The objective of this research is to study the effect of foundation soil on dynamic stability, including liquefaction, of embankment dams, through numerical illustration using FLAC<sup>3D</sup> and PLAXIS geotechnical softwares. An embankment dam may rest on a loose alluvium deposits for which it can accommodate the foundation deformation. The loose foundation soil, when exposed to cyclic load as in earthquakes, responds adversely from a relatively harder stratum. Sometimes such loose soil deposits amplify the bedrock ground motion inducing a problem on stability of the embankment. Such cases need to be considered in resting an embankment in a thick alluvium deposits, particularly in earthquake prone zones. If the loose soil deposits are removed to a relatively stiffer soil underneath or if the depth of such soils is reduced, the adverse effect mentioned above may be reduced. For the purpose of studying the effect of foundation soil on dynamic stability of embankments, a 2-D dynamic analysis of site soil and an overlying embankment is done. FLAC<sup>3D</sup> version 3 and PLAXIS 8.2 professional version geotechnical softwares were chosen in the numerical modeling framework. Soil properties were reasonably taken from the results of other available site investigation studies. A two dimensional mesh was created to represent the topographic and geometric constraints of the problem. Linearly elastic perfectly plastic constitutive model was implemented to model the soil behavior in both FLAC<sup>3D</sup> and PLAXIS geotechnical softwares. The results of 2-D dynamic numerical analyses in the forms of acceleration, displacement, strain, stress and pore pressure are presented and compared. The analysis result reveals that for an embankment resting on a loose foundation, the displacement, acceleration, stress, strain and porewater pressure values are higher than that of embankment founded on relatively stiffer ground in both FLAC<sup>3D</sup> and PLAXIS softwares. The higher displacement, acceleration, strain and stress levels calculated for an embankment founded on a loose ground can be attributed as a cause of poor performance of such embankments when earthquakes happen. From the result of the study, it can be seen that loose foundation soils induce dynamic stability problem on embankment dams. This shows the necessity of foundation soil investigation for dynamic stability while resting embankment dams on loose foundation soils as in alluvial deposits.

## 1. INTRODUCTION

### 1.1. General

Dams are artificial barriers constructed to retain water for different purposes. A dam may be concrete or embankment type. Embankment dam is a dam constructed out of natural (soil) material by mechanical compaction. Embankment dams may be classified as earth fill and/or rock fill depending on the percentage of fill material. According to ICOLD, (International Commission on Large Dams) more than 80 % of large dams (dams exceeding 15 m in height) constructed all over the world are of embankment type [1].

Embankment dams are subjected to both static and dynamic type loads. The retained water load, self-weight of the dam and uplift pressure through the foundation are the static loads acting on embankment dams. Earthquakes make the greater portion of dynamic load acting on embankment dams. In design and analysis of embankment dams, both types of loads need to be considered while analyzing the deformation, stress, porewater pressure buildup and failure responses of the dam. Earthquakes may induce sudden built up in pore water pressure and reduce the effective stress to zero. This causes liquefaction [1, 2].

Embankment dams are adaptable to a wide range of foundation conditions. This is one advantage, among others, of embankment dams over concrete dams. In areas where there is thick deposit of loose soil, embankment dams are favored to accommodate for the foundation deformation [2]. However, such thick deposits of soft soil (alluvium deposit) may induce problems on the dynamic stability of dams when earthquakes happen. Thick deposit of soft soil may even amplify the bedrock ground motion and trigger liquefaction [2]. Failure due to soft foundation soil condition has been observed in buildings resting on a soft ground [3].

### 1.2. Statement of the problem

Thick deposits of alluvial soils may be left as they are in construction of embankment dams due to economic or other reasons. Only the site where the core of the dam rests may be excavated deeper to the bedrock or provided with a curtain. Removing or reducing the alluvium deposit thickness to some extent helps to reduce the liquefaction potential of the foundation soil during earthquake loading. Therefore, the degree to which loose foundation soil is affecting dynamic stability of embankment dams should be thoroughly studied and considered in design and analysis.

### 1.3. Objectives of the study

This study intends to determine the effect of foundation soil on possible cyclic load induced instability (liquefaction) of embankment dams due to earthquake loading. To do so, a numerical illustration is done using the *FLAC<sup>3D</sup>* and *PLAXIS* geotechnical softwares incorporating the following parameters carefully.

- Soil formation under the embankment dam
- Soil properties
- Cyclic loading to represent earthquake load

To estimate;

- Deformation
- Effective vertical stress on embankment dams and foundation soil
- Pore pressure

The outcomes of the numerical illustration are then compared to each other based on the foundation soil type.

#### **1.4. Scope of the study**

This study is entirely dependent on outcomes of the typical numerical illustrations done to observe the cyclic load induced instability and liquefaction of embankments from the two geotechnical softwares. A homogeneous earthfill embankment dam is considered in the numerical illustration. The same section of embankment is analyzed separately with the two geotechnical softwares in three cases each in the numerical illustration. The embankment is considered while it rests on loose foundation soil, relatively stiffer foundation soil and layered foundation soil.

The paper is organized in six chapters. The first chapter is the introduction. Literature review on liquefaction of embankment dams and numerical modeling is presented on the second chapter. Numerical modeling basis and procedure is discussed on the third chapter. The fourth chapter is devoted to the numerical illustration where static and dynamic analysis of an embankment dam is carried out. The same section of dam resting on different foundation soils (loose alluvial deposit, relatively stiffer deposit and layered) is analyzed when subjected to cyclic loading.

The first case is when the dam rests on thick alluvium deposit and the second case is when the alluvium deposit is excavated and removed to the relatively stiffer formation. The third case considers a dam resting on layered foundation of three layers. The results of the analyses are compared to each other from stress, strain and liquefaction perspective.

On the fifth chapter, the results of the numerical examples are discussed. The findings derived from the project, conclusions and recommendations are summarized on the sixth chapter.

© GSJ

## **2. LITERATURE REVIEW**

### **2.1. Embankment dams**

#### **2.1.1. General**

Embankment dam is a dam constructed from natural materials (soil) excavated or obtained close by. Upstream and downstream slopes are provided. Embankment dams consume large amount of construction material (soil and rock) due to their wide cross section.

About 90 percent of dams built all over the world are of embankment type [1]. They are technically easy and economical compared to concrete dams. Embankment dams are adaptable to wide range of foundation conditions. From competent rock formation to soft alluvium deposits, embankment dams are widely employed because they can accommodate the different site condition.

The following is summary of the main advantages of embankment dams over concrete dams [1].

- Suitable to sites of wider cross section;
- Flexibility to a broad range of foundation conditions;
- Use existing naturally available material usually found around the construction site;
- The construction process is highly mechanized and is effectively continuous;
- Cost effective when compared to concrete dams;
- Embankment dams can accommodate foundation deformation without major failure.

#### **2.1.2. Embankment dam types and characteristics**

Embankment dams are broadly classified as earthfill and/or rockfill. The classification scheme is inclusive. All embankment dams use both earth (soil) and rock. The classification is based on the percentage of material usage. The material used available is compacted mechanically without any artificial cementing material [1].

- Earthfill: more than 50 percent of material used is soil.
- Rock fill: more than 50 percent of material used is rock.

#### **2.1.3. Foundation investigations**

The advantage of being adaptable to different foundation conditions, sometimes, makes embankment dams vulnerable to liquefaction due to cyclic loading [2].

Usually foundation competence of the dam site is assessed in terms of stability, bearing capacity, compressibility or deformability and permeability. The following foundations characteristics are observed in stiff and soft formation [1].

##### **(a) Dams on Competent Stiff Clays and Rock**

Seepage is not a big problem in extensive and uniform deposits of competent rock and clay. Liquefaction also may not be problems as it usually happens in saturated loose sand.

### **(b) Dams on Pervious Foundations**

Seepage problems are common where a dam is to be founded on a relatively pervious foundation as alluvium deposit. In a high proportion of such instances, the soil conditions are very complex, with permeability and potential liquefaction.

#### **2.1.4. Seismicity**

Dynamic loads as in earthquakes need to be considered in the design of embankment dams. Especially in earthquake prone areas, the effect of the dynamic disturbance on deformation and potential liquefaction should be thoroughly studied.

Seismic activity generates dynamic loads due to the inertia of the dam and the retained body of water. In addition, it induces increase in porewater pressure in foundation and embankment itself [1].

A seismic event can be characterized by its magnitude and its intensity, as explained below:

**Magnitude:** a measure of the energy released due to the earthquake. It can be described with the Richter Scale, ranging from  $M=1.0$  to  $M=9.0$ . The damage expected due to an earthquake on embankment dams increases in parallel to the magnitude.

**Intensity:** it is a measure of the destruction of seismic shaking attaching to an event. Intensity varies with position and distance from the epicenter.

In design procedure, seismic event is usually described in the following terms.

**Maximum Credible Earthquake (MCE):** is the event forecasted to produce the harshest level of ground motion possible for a specific site.

**Safety Evaluation Earthquake (SEE):** is the design ground motion for which the safety of a dam must be assured. SEE is usually defined as a proportion of the MCE.

Ground motions due to earthquakes can be described in terms of acceleration, velocity and displacement. Peak ground acceleration (PGA) generally expressed as a proportion of gravitational acceleration,  $g$ . The duration of the earthquake has been found more detrimental than the PGA values when earthquake damage is considered [1].

#### **2.1.5. Seismic loading**

This is known as equivalent static loads, dynamic loads can be approximated by inertia forces triggered by ground motion. In Pseudostatic inertia forces are calculated in terms of the acceleration value selected for design and used as equivalent to additional static loads. This method is generally conservative. In analysis of dams of special interest, numerical methods need to be employed to comprehensively analyze the dam including porewater pressure distribution analysis.

##### 2.1.5.1. Pseudostatic analysis

The ratios of PGA to gravitational acceleration in horizontal and vertical directions are generally used to express the strength of an earthquake. The representative seismic coefficients,  $\alpha_h$  in horizontal direction and  $\alpha_v$  in the vertical direction, are then applied in design where

$\alpha_h$  and  $\alpha_v$  are seismic coefficient in the horizontal and vertical direction respectively.

Inertia forces triggered with the mass of a dam structure are expressed in terms of the horizontal and vertical seismic acceleration coefficients,  $\alpha_h$  and  $\alpha_v$  respectively, and gravitational acceleration,  $g$ , thus:

Horizontal forces =  $\alpha_h \times m$ .....2.1

Vertical forces =  $\alpha_v \times m$ ..... 2.2

Where  $m$  is static mass of the dam

For initial analysis, they are assumed to operate through the centroid of the mass to which they are considered to apply.

#### 2.1.5.2. Dynamic response analysis

The simplifications made in pseudostatic analysis are many. Among these, complex problems of dam-foundation and dam-reservoir interaction and the load response of the dam itself are neglected. These interactions are of great importance. Generally, they modify the dynamic properties of the dam and consequently may significantly affect its load response.

In dynamic response analysis method, the dam is discretized as a two or three-dimensional finite element system, the reservoir being regarded as a continuum. The foundation zone is generally idealized as a finite element system equivalent to a viscoelastic half-space. The complexities of such an approach are evident.

It has been suggested that the application of more rigorous methods, such as dynamic analysis, in preference to the simplistic pseudostatic approach is appropriate if the anticipated PGA will exceed 0.15 g [1].

#### **2.1.6. Seismic damage to embankment dams**

Earthquake damage to embankments, which could potentially lead to catastrophic failure, can be summarized in the following modes:

- Shear displacement;
- Slope Instability;
- Foundation instability;
- Liquefaction
- Flow slides;
- Volume reduction of the embankment fill;
- Differential displacements
- Internal cracking ;
- Failure of ancillary structures, including spillways, outlet tunnels and culverts;
- Valley slopes Instability.

Liquefaction and a flow slide as a result of pore pressure generation and soil densification is effectively limited to loose, coarser soils such as

sands [4].

### 2.1.7. Liquefaction of dam embankments and foundations

Liquefaction is generally defined as loss of shear strength of a soil. Liquefaction may be associated to different phenomena including dynamic disturbance. The following types of liquefaction are associated with dynamic loading [4].

**“Cyclic Liquefaction”** is a temporary liquefaction, where the cyclic loading causes shear stress reversal and an initial liquefaction (zero effective stress) condition develops temporarily.

**“Cyclic Mobility”** is a form of temporary liquefaction where the shear stresses are always greater than zero. Saturated sands, silty sands, and gravelly sands are susceptible to liquefaction.

#### 2.1.7.1. The effects of cyclic loading

In loose granular soils, cyclic loading causes densification due to soil grain rearrangement. If the soil is saturated and undrained, the densification is accompanied by porewater pressure development. The pore water developed decreases the effective stress up to zero and causes liquefaction.

The phenomenon as illustrated in the figure below illustrates the reduction in void ratio causes increase in porewater pressure and decrease in effective stress.

Porewater pressure is built up gradually with a number of cyclic loading. By the time the porewater pressure equals to the vertical stress, effective stress will be equal to zero and liquefaction occurs [2].

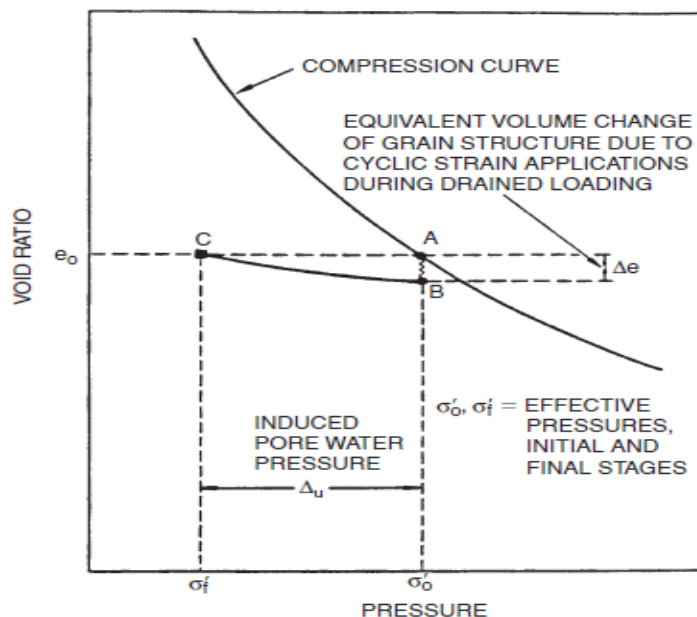


Figure 2. 1 Schematic illustration of mechanism of pore pressure generation during cyclic loading (Seed & Idriss 1982; USNRC, 1985).

## 2.2. Numerical analysis

Numerical methods generally work by discretizing a defined continuum. Finite element, finite difference and boundary element methods are some numerical methods of analysis applicable to embankments [3].

### 2.2.1. Finite element methods

In finite element method the response of the embankment and foundation are described by the response of the nodal points of the discretized elements.

For an element of four nodes ( quadrilateral element) nodal point displacements can be given as  $\{S^T\}=\{u_1,u_2,u_3,u_4,v_1,v_2,v_3,v_4\}$  in two dimensions as shown in Figure 2.2 below.

Where;  $u_i$ = nodal point displacement in the x-direction

$v_i$ = nodal point displacement in the y-direction

The displacements for any point in the element can be expressed in the following form.

$$\{V\}=[N] \{S\} \dots\dots\dots 2.1$$

Where  $[N]$  is a matrix of shape functions.

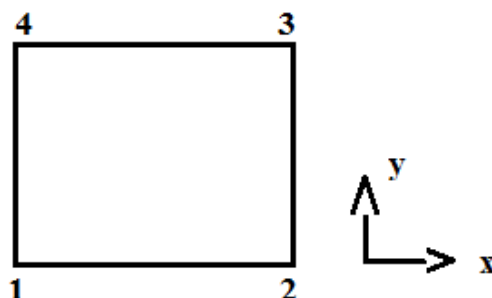


Figure 2. 2 Quadrilateral element

The strain displacements matrix,  $[B]$ , allows the strains to be determined from the nodal point displacements

$$\{\varepsilon\}=[B]\{S\} \dots\dots\dots 2.2$$

and the stress strain matrix  $[D]$ , relates stresses to strains:

$$\{\sigma\}=[D]\{\varepsilon\} \dots\dots\dots 2.3$$

The equations of motion for the element can then be written as;

$$[m_e]\{S''\}+[c_e]\{S'\}+[k_e]\{S\}=\{Q(t)\} \dots\dots\dots 2.4$$



Where  $[m_e]$  is mass matrix of an element

$[c_e]$  is damping matrix of an element

$[k_e]$  is stiffness matrix of an element

$\{S\}$  is displacement vector of an element

$\{S'\}$  is velocity vector of an element

$\{S''\}$  is acceleration vector of an element and

$Q(t)$  is elemental nodal point force

The global equations of motion is then written as,

$$[M]\{U''\} + [C]\{U'\} + [K]\{U\} = \{Q(t)\} \dots\dots\dots 2.5$$

Where  $[M]$  is the global mass matrix,

$[C]$  is the global damping matrix,

$[K]$  is the global stiffness matrix,

$\{U\}$  is the global nodal point displacement vector

$\{U'\}$  is the global nodal point velocity vector

$\{U''\}$  is the global nodal point acceleration vector and

$\{Q(t)\}$  the global nodal point force vector.

## 2.2.2. Finite difference methods

In finite difference method, the solutions are computed at specific discrete points called nodes.

The equations of motion for a mass-dashpot-spring system may be expressed, in matrix notation, as;

$$[M]\{u''\} + [C]\{u'\} + [K]\{u\} = \{P\} \dots\dots\dots 2.6$$

Which is similar with finite element equations as in the Eq.(2.5) . The difference is that the derivatives in the governing equation are written in finite difference method.

## 2.3. Constitutive models

There are a number of constitutive models, which can be used to define material behavior under different load cases and material behavior.

The following are among them, which are used in this project.

### 2.3.1. Elastic model

The Hooke law is the governing linear relation in elastic model. An increase in strain generates an increase in stress. This model is the simplest representation of material behavior under load.

$$\Delta\sigma_{ij} = 2G\Delta\epsilon_{ij} + \alpha_2 \Delta\epsilon_{kk} \delta_{ij} \dots\dots\dots 2. 7$$

Where,  $\delta_{ij}$  is the Kroenecker delta symbol,

$\alpha_2$  is a material constant related to the bulk modulus, K, and the shear modulus G.

$\sigma_{ij}$  and  $\epsilon_{ij}$  are stress and strain values. New stress values are then obtained from the relation.

Stress value can be then computed from existing values from;

$$\sigma_{ij}N = \sigma_{ij} + \Delta\sigma_{ij} \dots\dots\dots 2.8$$

### 2.3.2. Mohr Coulomb Plasticity Model

According to Mohr's theory, failure along a plane in a material occurs by a combination of normal and shear stresses, not by either of them alone.

Mohr defined the functional relation between normal stress ' $\sigma$ ' and shear stress ' $s$ ' as;

$$s = c + \sigma \tan \phi \dots\dots\dots 2.9$$

Where  $c$  is cohesion and  $\phi$  is the angle of friction of the soil. The above equation is referred to as the Mohr-Coulomb failure criteria. In saturated soils, the stress carried by the soil solids is the effective stress and so the above equation has to be modified to effective stress [5].

Based on the Mohr-Coulomb failure criterion, the Mohr-Coulomb constitutive model is generated incorporating the failure Mohr's envelop.

### 2.3.3. Finn Model

Finn model is used to generate dynamic porewater pressure distributions. Martin (1976) supposed that it is the grain rearrangement rather than grain volume change that takes place, thus the volume of the void space decreases under constant confining stress. If the voids are filled with fluid, then the pressure of the fluid increases and the effective stress acting on the grain matrix decreases. The externally applied stress is then gradually transferred from soil grains to the fluid that increases the fluid pressure.

Martin et al (1976) supply the Eq. (2.10) that relates the increment of volume decrease ( $\Delta\epsilon_{vd}$ ) to the cyclic shear strain amplitude ( $\gamma$ ), where  $\gamma$  is presumed to be the engineering shear strain.

$$\Delta\epsilon_{vd} = D_1 (\gamma - D_2 \epsilon_{vd}) + \frac{D_3 \epsilon_{vd}^2}{\gamma + D_4 \epsilon_{vd}} \dots\dots\dots 2.10$$

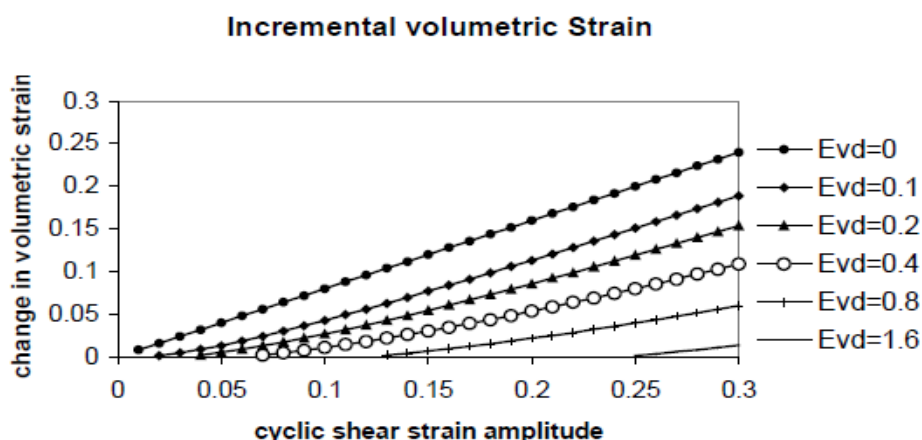


Figure 2. 3 ( Martin 1976) volumetric strain curves for the sand with  $D_1=0.8$ ,  $D_2=0.79$ ,  $D_3=0.45$  and  $D_4=0.7$

Eq. (2.10) involves the accumulated irrecoverable volume strain  $\epsilon_{vd}$  in such a way that the change in volume strain decreases as volumetric strain increases. Presumably,  $\Delta\epsilon_{vd}$  should be zero if  $\gamma$  is zero; this implies that the constants are related as follows:  $D_1 * D_2 * D_4 = C_3$ .

Alternatively, Byrne (1991) proposed a simpler formula for the determination of  $\Delta\varepsilon_{vd}$ ;

$$\left(\frac{\Delta\varepsilon_{vd}}{\gamma}\right) = B_1 \exp\left(-B_2 \cdot \left(\frac{\varepsilon_{vd}}{\gamma}\right)\right) \dots\dots\dots 2.11$$

Where usually  $B_2 = \frac{0.4}{B_1}$  Therefore, the above equation involves only one independent constant. According to (Byrne 1991) the only independent variable can be determined by;

$$B_1 = 8.7(N_1)_{60}^{-1.25} \dots\dots\dots 2.12$$

Where  $(N_1)_{60}$  normalized N where N is the standard penetration resistance, the number of blows required to achieve the last 30 cm of penetration in SPT. Finally, these pore pressure models are inserted into the Mohr-Coulomb plasticity model. The Finn model is constructed following the above-mentioned rule and relating the volume change to porewater generation.

## 2.4. Cyclic stress approach of evaluating liquefaction

In Cyclic Stress approach, the level of excess pore pressure required to initiate liquefaction is dependent on amplitude and duration of earthquake-induced cyclic loading. This method assumes that excess pore pressure generation is essentially related to the cyclic shear stresses. Seismic loading, thus, can be expressed in terms of cyclic shear stresses as in the Eq (2.13)

$$\tau_{cyc} = 0.65 * \tau_{max} \dots\dots\dots 2.13$$

Where  $\tau_{max}$  is the maximum shear stress.

Cyclic shear stress is usually normalized by the initial effective overburden pressure to produce a cyclic stress ratio (CSR) as in Eq(2.14).

$$CSR = \frac{\tau_{cyc}}{\sigma'_{vo}} \dots\dots\dots 2.14$$

Defining the maximum shear stress as,

$$\tau_{max} = \left(\frac{a_{max}}{g}\right) \sigma'_{vo} rd \dots\dots\dots 2.15$$

The cyclic stress ratio equation above can then be written as;

$$CSR = 0.65 \left(\frac{a_{max}}{g}\right) \left(\frac{\sigma'_{vo}}{\sigma'_{vo}}\right) rd \dots\dots\dots 2.16$$

Where  $a_{max}$  is peak horizontal acceleration at the ground surface,

$g$  is the acceleration of gravity,

$\sigma_{vo}$  and  $\sigma'_{vo}$  are total and effective vertical overburden stresses, respectively and

$rd$  is the stress reduction coefficient.

Finally, the plot of CSR versus  $(N_1)_{60}$  defines boundaries of liquefaction susceptible considering the clean sad base curve earthquakes and fine contents. This methodology has become a standard of practice in many countries for evaluating liquefaction resistance of soil (7).

The SPT is the most commonly used in situ test for characterization of liquefaction resistance. The number of blows required to achieve the

last 30 cm of penetration is taken as the standard penetration resistance, N. The N value is a function of the soil type, confining pressure, and soil density, but is also influenced by the test equipment and procedures. Generally cyclic shear stress required to initiate liquefaction increases with increase in effective confining pressure.

© GSJ

### 3. MODELING, MATHEMATICAL BASIS AND PROCEDURES

#### 3.1. Introduction

This project work is entirely dependent on the results of numerical illustrations using the FLAC<sup>3D</sup> and PLAXIS geotechnical softwares. Numerical analysis is performed in three cases using the FLAC<sup>3D</sup> and three cases using PLAXIS softwares. Below, the modeling of the profiles, mathematical basis and procedures followed to find results are discussed in detail.

#### 3.2. Preliminary data for analysis

The embankment dam considered in all cases is a homogeneous earthfill dam of 20 meters height. The property of the dam fill material is representatively considered as given in the table below.

*Table 3. 1 embankment fill property*

Property	Embankment
bulk modulus (KPa)	3.30E+04
shear modulus (KPa)	7.50E+03
cohesion ( KPa )	10
poissons ratio (v)	0.3
density (kg/m3)	1700
porosity	3.00E-01
Permeability (m/s)	1.00E-08

##### 3.2.1. Case one: dam resting on silty sand foundation soil

The dam is analyzed when resting on a soft silty sand foundation soil using both the FLAC<sup>3D</sup> and PLAXIS geotechnical softwares. The foundation soil is modeled up to a depth of 15 to 20 meters, together with the dam, for analysis. The property of the silty sand foundation soil is summarized in the table below. The soil properties are carefully assumed to represent actual site soil conditions in all the three foundation soil conditions.

*Table 3.2 silty-sand foundation soil property*

Property	Silty Sand Foundation Soil
bulk modulus (KPa)	7.60E+04
shear modulus (KPa)	1.50E+04
cohesion ( KPa )	30
poissons ratio (v)	0.38
density (kg/m3)	1700
porosity	0.3
Permeability (m/s)	1.00E-06

### 3.2.2. Case two: dam resting on silty clay foundation

On the second case, the dam is resting on a relatively stiffer silty clay foundation soil. The foundation soil is modeled together with the dam up to 15 to 20 meters depth for the analysis using both FLAC<sup>3D</sup> and PLAXIS geotechnical softwares. The properties of silty clay foundation soil are given in the table below.

Table 3.3 silty-clay foundation soil property

Property	Silty clay Foundation Soil
bulk modulus (KPa)	1.26E+05
shear modulus (KPa)	6.50E+04
cohesion ( KPa )	50
poissons ratio (v)	0.28
density (kg/m3)	1900
porosity	0.3
Permeability (m/s)	1.00E-08

### 3.2.3. Case three dam resting on layered foundation

The third case is analysis of the same dam section as case one and case two while it rests on a layered soil of three layers. The foundation is modeled up to 15 meters depth. Each layer is of 5 meters thickness. The first layer is silty sand soil. Underneath the silty sand soil there exists a silty clay soil underlie by clay soil. The analysis is done using FLAC<sup>3D</sup> and PLAXIS and compared with the above two cases respectively. Below in the table is the summery of the properties of each soil layer of foundation.

Table 3.4 layerd foundation soil property

Property	Foundation Soil		
	Silty sand	Silty clay	Clay
bulk modulus (KPa)	7.60E+04	1.26E+05	3.00E+05
shear modulus (KPa)	1.50E+04	6.50E+04	8.00E+04
cohesion ( KPa )	30	50	50
poissons ratio (v)	0.38	0.28	0.25
density (kg/m3)	1700	1900	1900
porosity	0.3	0.3	0.2
Permeability (m/s)	1.00E-06	1.00E-08	1.00E-08

### 3.3. Cyclic load characteristics

To model earthquake loading on embankment dams, two methods are used in the numerical illustrations.

In FLAC<sup>3D</sup>, the earthquake loading is modeled using a user defined harmonic cyclic load. FLAC<sup>3D</sup> allows user defined, flacish, (FISH) models.

Users can define functions in a language that the FLAC<sup>3D</sup> can understand and the software supports such functions. The characteristics of the cyclic load are summarized in the table below. The characteristics of the harmonic load are selected to enable easy observation of the effect of the load on the embankment.

*Table 3.5 cyclic load characteristics*

Cyclic Load Characteristics	
load	1
amplitude	10
frequency	0.5
number of cycles	1

In numerical illustrations done using the PLAXIS geotechnical software, an available record of earthquake loading on PLAXIS software tutorial package is used. The file is available and fed to the analysis in a SMC (Strong Motion CD-ROM) format.

### **3.4. Modeling and analysis using the FLAC<sup>3D</sup>**

As mentioned above the FLAC<sup>3D</sup> is used in the analysis of case-one, case-two and case-three cases. The results of the three analyses are then compared to each other to study the effect of foundation soil type. The modeling and analysis in FLAC<sup>3D</sup> in all cases is same except that the foundation soil condition is different.

#### **3.4.1. Modeling the profile of the dam**

In order to carry out the analysis, first modeling of the actual embankment dam is necessary to perform with FLAC<sup>3D</sup> software. To model the dam, the following steps were performed:

1. Establishing boundary conditions to discretized the domain
2. Discretization: subdivision of the actual dam in to fine meshes with known dimension so that simulation of the dam can be achieved with FLAC<sup>3D</sup>.
3. Development of programs with notepad by using the coordinates of the meshes.

In order to carry out the solution for the required problems, the domain has to be discretized. Discretization of a given proposed geometry of dam section in to finite number of elements is performed following the steps hereunder.

1. The discretization must consider aspect ratio (i.e. minimum size divided by maximum size of the element). The aspect ratio should not be less than 0.2 [3].
2. Dynamic requirements must be satisfied.

Preparation of the soil mesh is an important step in numerical analysis. The mesh generation of z- axes is important since the input motion waves propagate on that axes.

In dynamic analysis of embankments, the dynamic property of the dam material and foundation has to be estimated accurately to find a good result. By considering the estimated shear wave velocity ( $V_s$ ) of the soil layers, the size of elements can be modeled. The discussion of implementing different element sizes in the mesh generation will be explained in the following pages.

### **Wave transmission**

Numerical distortion of the propagating wave can occur in dynamic analysis as a result of poor modeling. Both the frequency content of the input wave and the wave speed characteristics of the system affect the numerical accuracy of the wave transmission. It was shown that for accurate representation of wave transmission through a model, the spatial element size, ( $\Delta l$ ), must be smaller than approximately one-tenth to one-eighth of the wavelength associated with the highest frequency of the component of the input wave [6].

For this particular example; considering computer capacity and to reduce calculation time, the element size of the mesh is estimated to be five meter. A separate command is written on a notepad and called to the FLAC<sup>3D</sup> to model and analyze the dam both in static and dynamic analysis. The command to model and analyze statically and dynamically are written stepwise on the same notepad. The separate notepad command written to model and analyze the dam is given on appendix A. Static analysis exceeds the dynamic analysis so that the state of the dam is accurately modeled before the dynamic load. The Mohr-Coulomb model is used to evaluate the displacement, stress and acceleration response of the embankment. Dynamic porewater pressure generation of the embankment is also assessed with a separate program using Finn model.

### **3.4.2. Analysis of the dam**

FLAC<sup>3D</sup> understood a program written on notepad. It models and performs the analysis by reading the notepad written command. The procedure is as follows;

- Open FLAC<sup>3D</sup>
- Call the notepad file written to model and analyze the profile of the dam on the file menu
- Click inter

The analysis proceeds once the inter button is clicked on the keyboard. After the analysis is finished, the result is displayed on the FLAC<sup>3D</sup> window in graphs and figures. The displacement, acceleration, stress, strain, and porewater pressure responses can be viewed on the window using the plotitem button on the menu bar of the FLAC<sup>3D</sup>.

## **3.5. Modeling and analysis using the PLAXIS**

### **3.5.1. Modeling the profile of the dam**

On PLAXIS, the input data is fed to the software using data input menus on the tool and menu bar. The model generation follows the following step for all three cases except that the foundation soil property and section is changed.

- Open PLAXIS
- Open new project and give filename, model type and number of nodes for the element
- Draw the model of the dam using the geometry line input
- Assign the material property for each section ( dam and foundation) using material set button

### **3.5.2. Analysis of the dam and foundation**

Continue from the modeling, PLAXIS has commands for static and dynamic analysis of the dam and foundation. The procedure, continuing from the modeling is as bulletined below.

- Apply standard fixities for boundary condition using standard fixity button



- Generate the mesh using mesh generation button
- Assign the water table
- Generate porewater pressure and stress condition using the generate porewater pressure button
- Proceed to the calculation. The calculation is done in two stages. The dynamic load is called from a separate CD-ROM file for the analysis on dynamic analysis.
- The result can be seen informs of graphs and deformed mesh on the output window.

© GSJ

## 4. NUMERICAL ILLUSTRATIONS

### 4.1. Introduction

The purpose of this numerical illustration is to show the effect of foundation soil on dynamic stability and liquefaction of embankment dams. To do so, the site soil characteristics are carefully selected while simplifications on the section of the dam and cyclic load characteristics are made as discussed on chapter three.

### 4.2. Numerical example using PLAXIS

A dam of 20 meters height is analyzed for an earthquake when resting on three different types of foundation soils.

1. Three layered foundation soil of 5 meters thick each
2. Silty sand foundation soil of 15 meters thick
3. Silty clay Foundation soil of 15 meters thick

Earthquake load was applied in the form of acceleration time history. Linearly elastic constitutive model is used to model the dynamic response of the embankment and foundation. The response in terms of deformation, stress and excess porewater pressure is presented below. Liquefaction is not supported under PLAXIS version eight.

The analysis result show that embankment resting on soft layer (silty sand) deformed more than embankment resting on relatively stiffer soil (silty clay). The deformation on the embankment resting on foundation of three soil layers is minimum. This may be due to the fact that the weighted stiffness of the three layers is greater than the other two foundation soil conditions i.e. silty sand and silty clay foundations.

The results of the dynamic analysis of the three cases when exposed to the same magnitude of dynamic loading is shown and discussed below.

#### 4.2.1. Analysis procedure and results of dam resting on a silty sand foundation (Case-one)

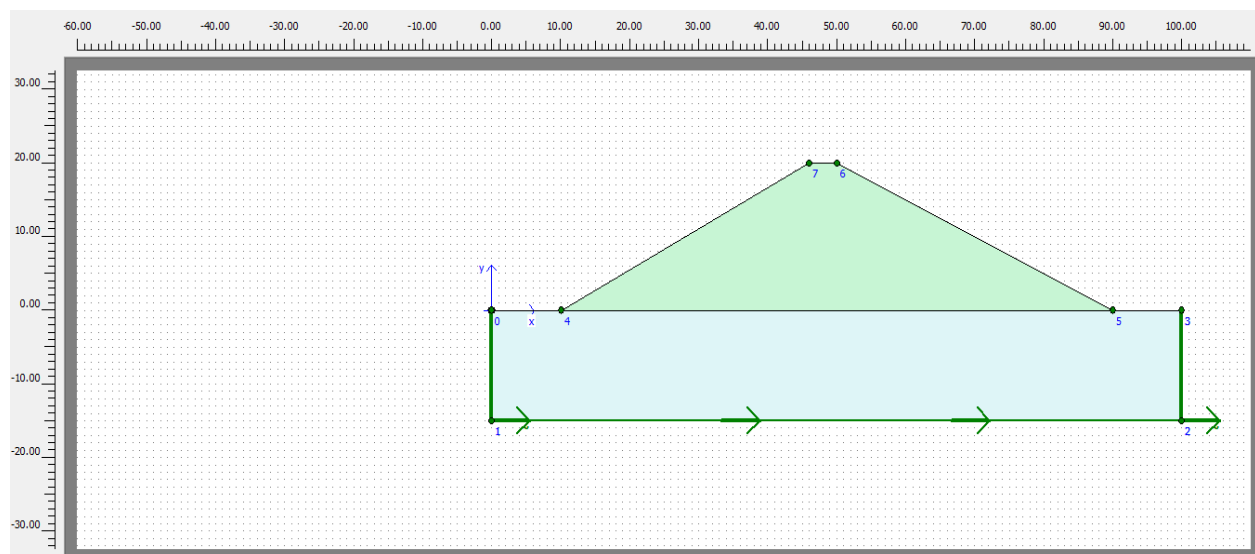


Figure 4. 1 Dam and foundation cross-section 1

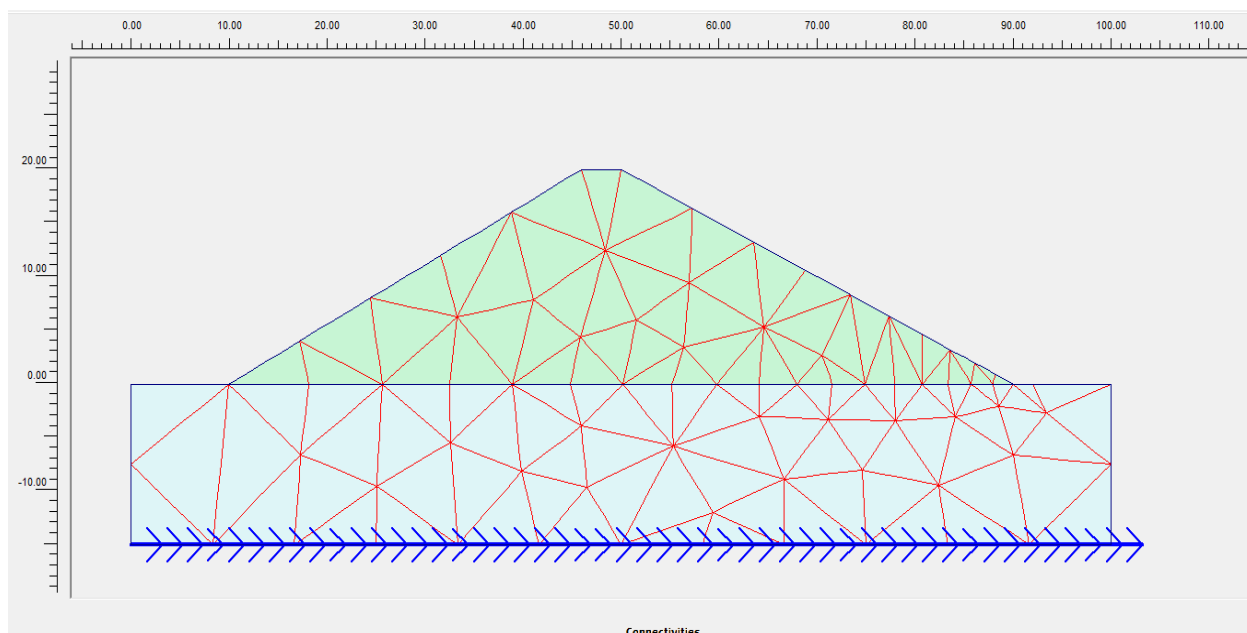


Figure 4. 2 Mesh generation

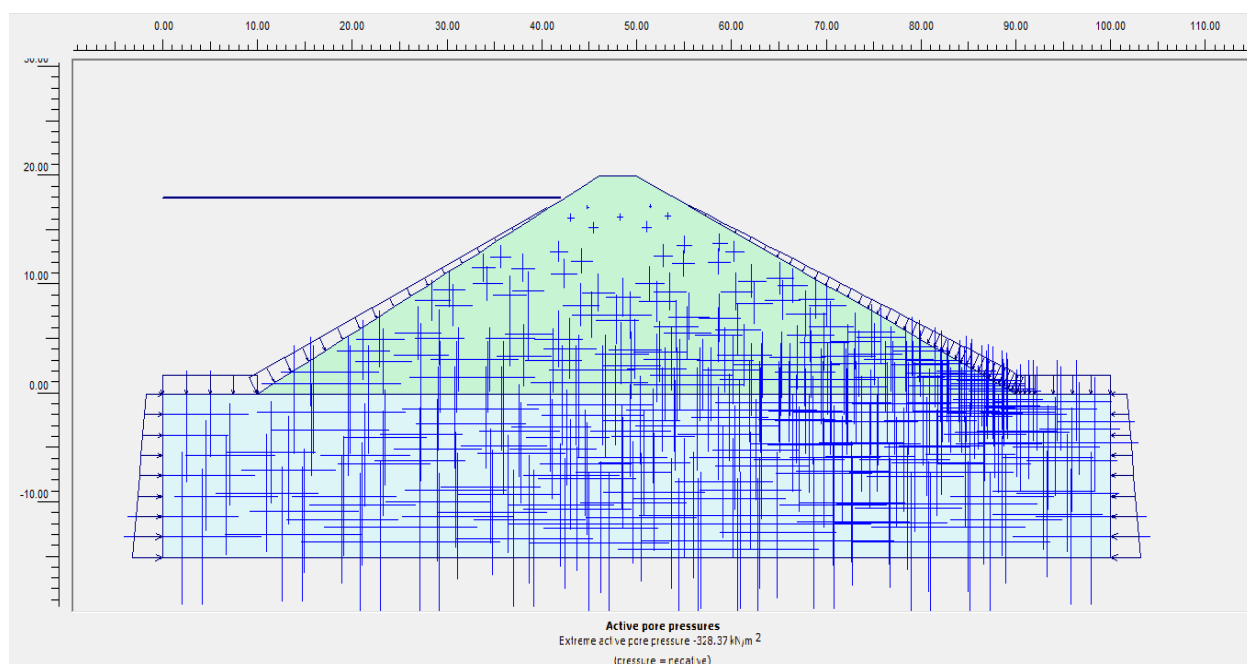


Figure 4. 3 Water table (porewater pressure distribution)

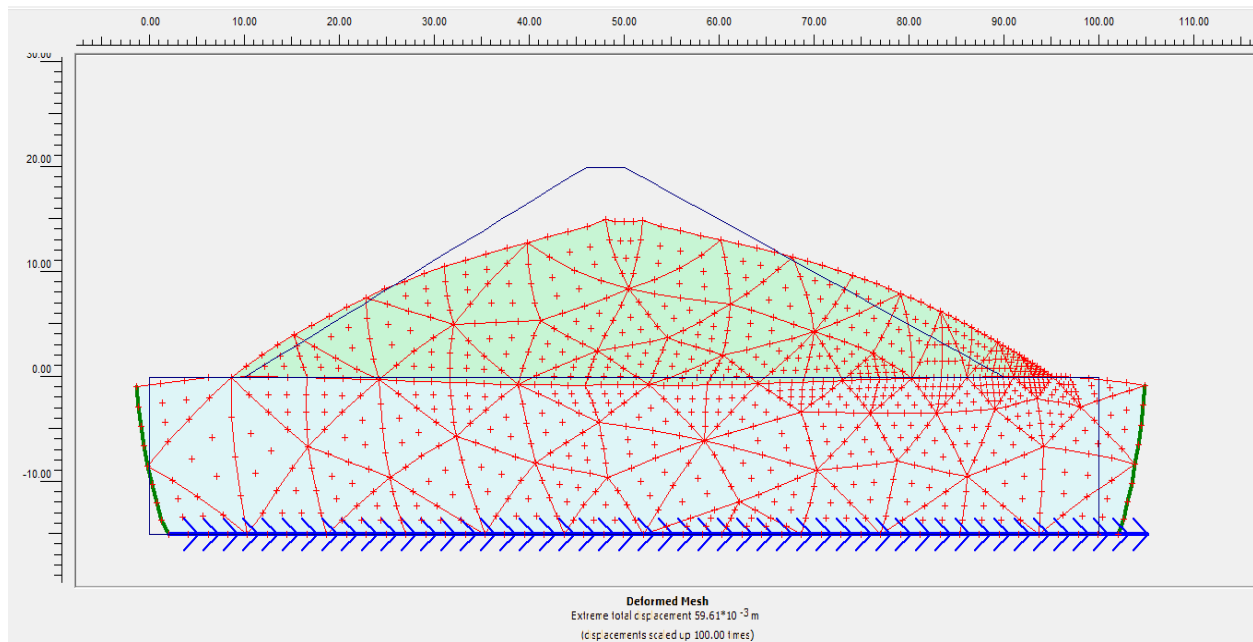


Figure 4. 4 Deformed mesh (maximum displacement 59.61 mm)

#### 4.2.2. Analysis procedure and results of dam resting on a silty clay foundation (Case-two)

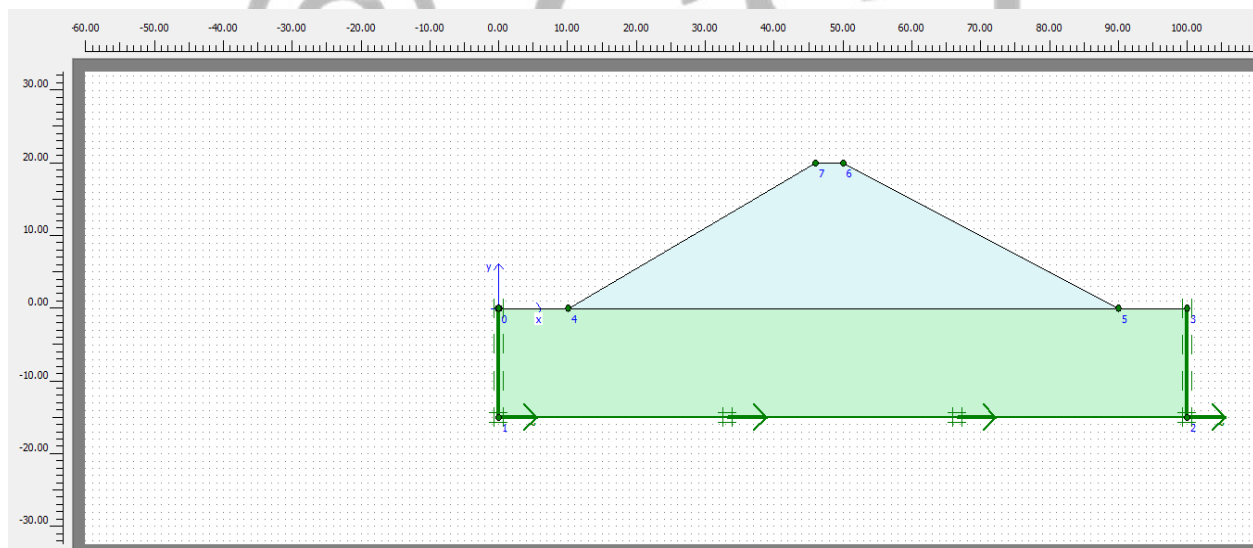


Figure 4. 5 dam and foundation cross-section 2

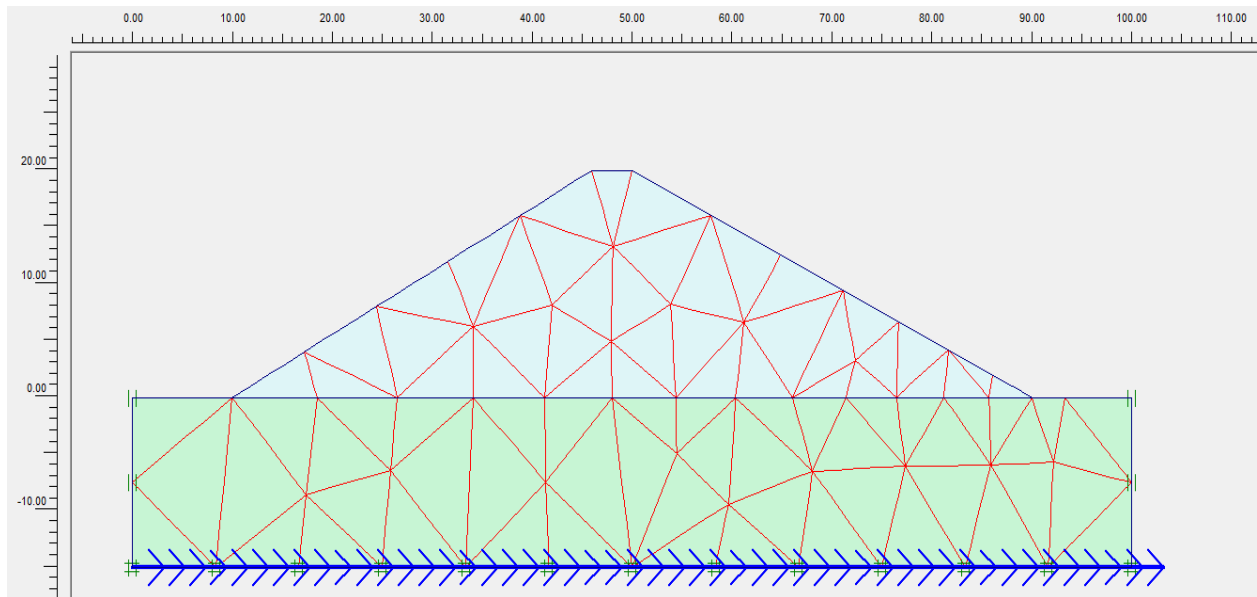


Figure 4. 6 Mesh generation

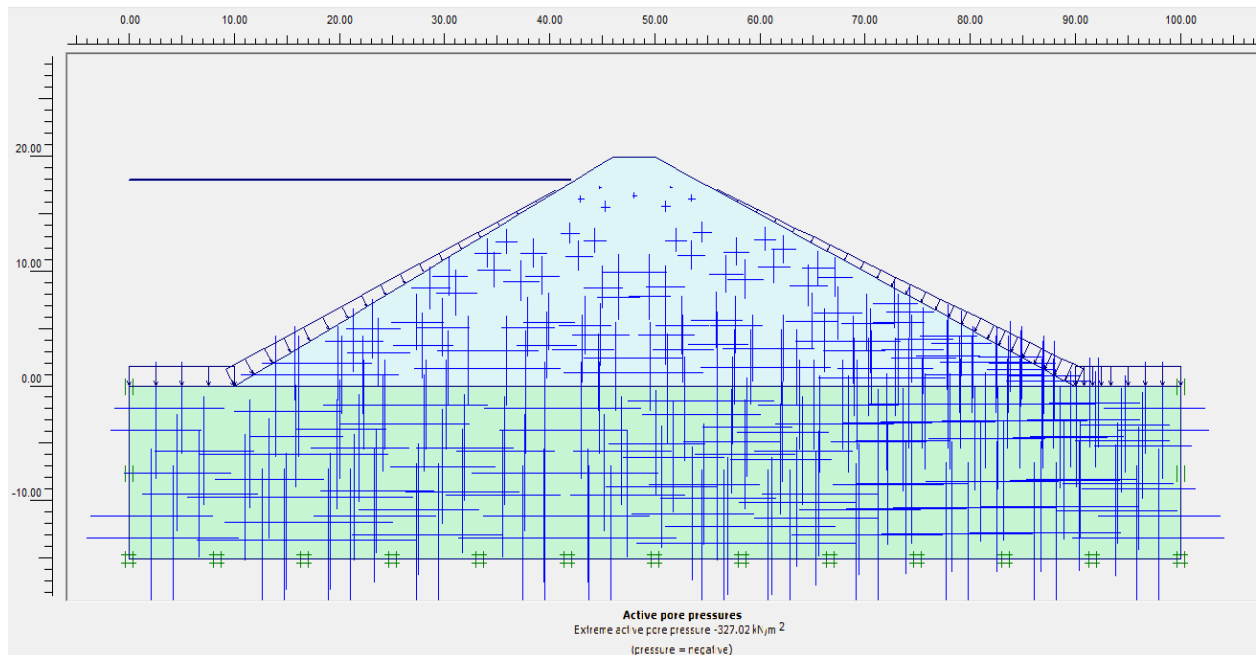


Figure 4. 7 Water table (porewater pressure distribution)

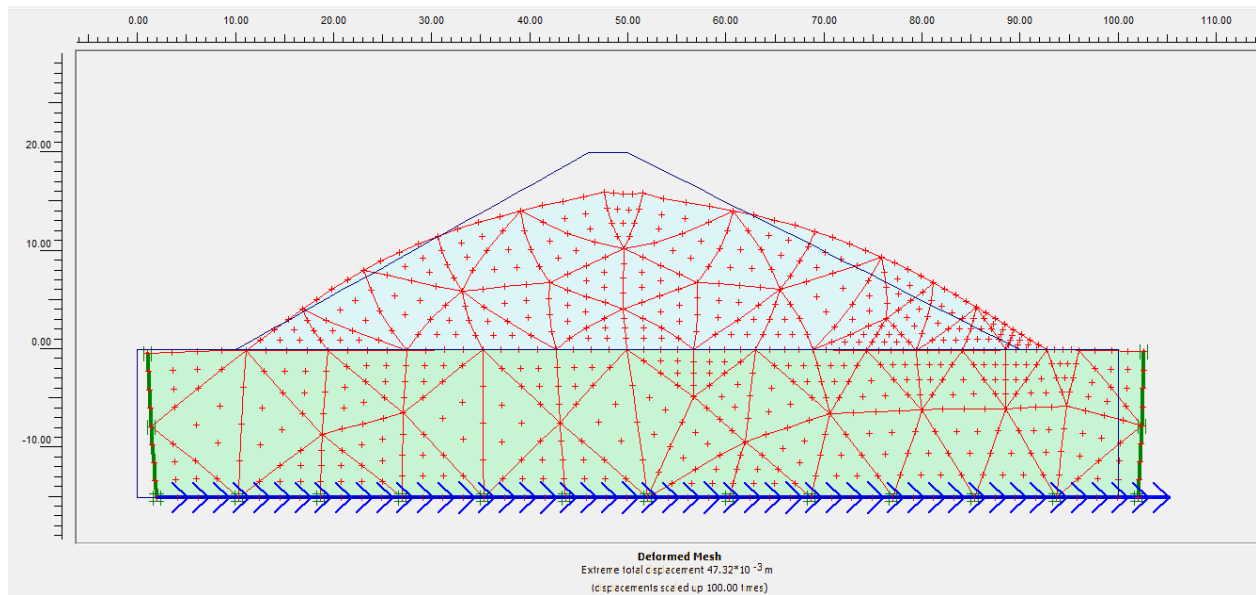


Figure 4. 8 Deformed mesh (maximum displacement 47.32 mm)

#### 4.2.3. Analysis procedure and result of dam resting on a layered foundation (case-three)

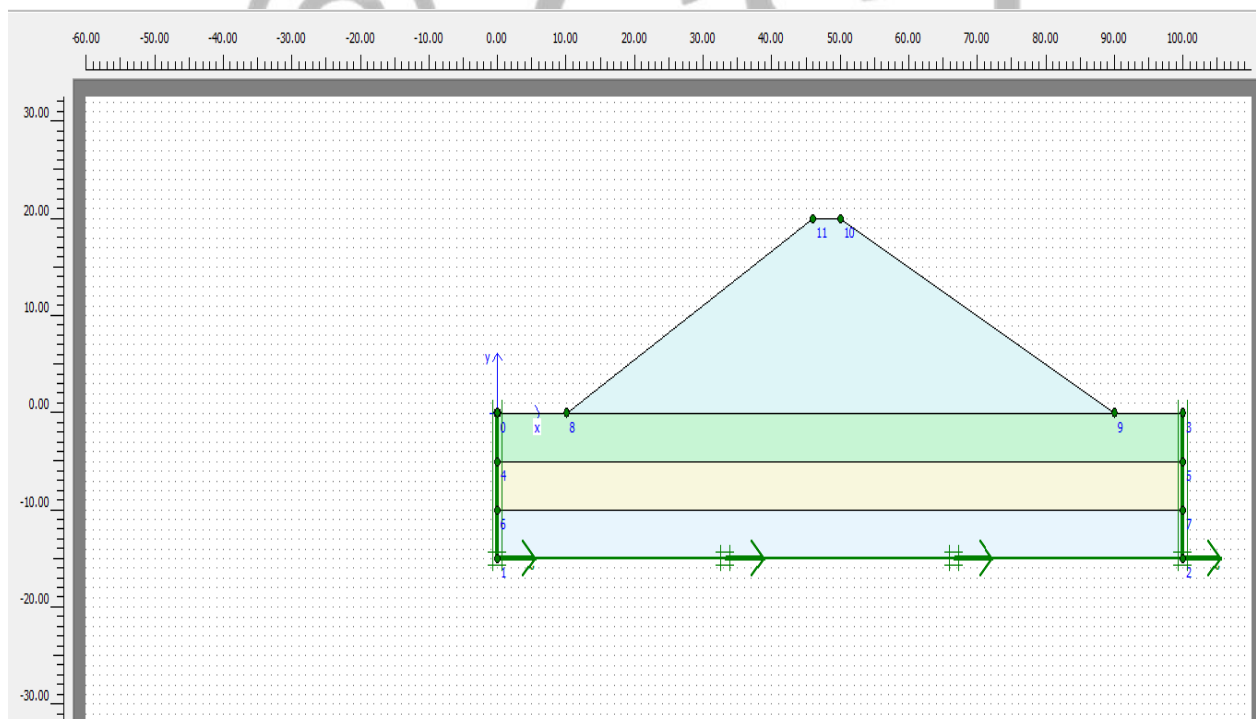


Figure 4. 9 Dam and foundation cross-section 3

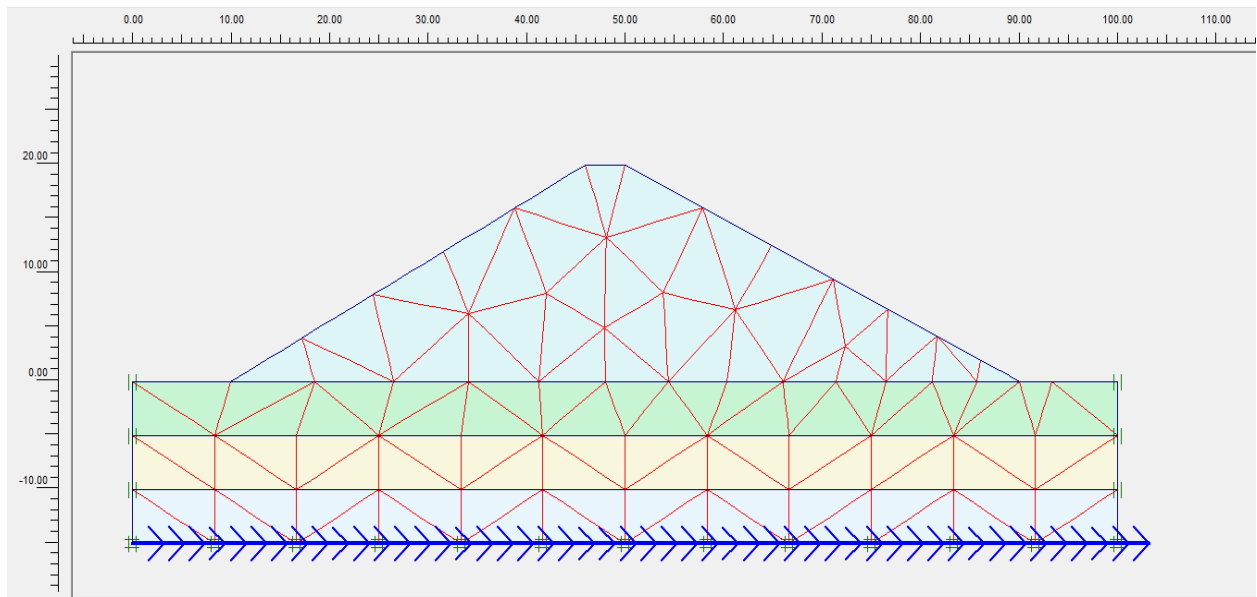


Figure 4. 10 Mesh generation

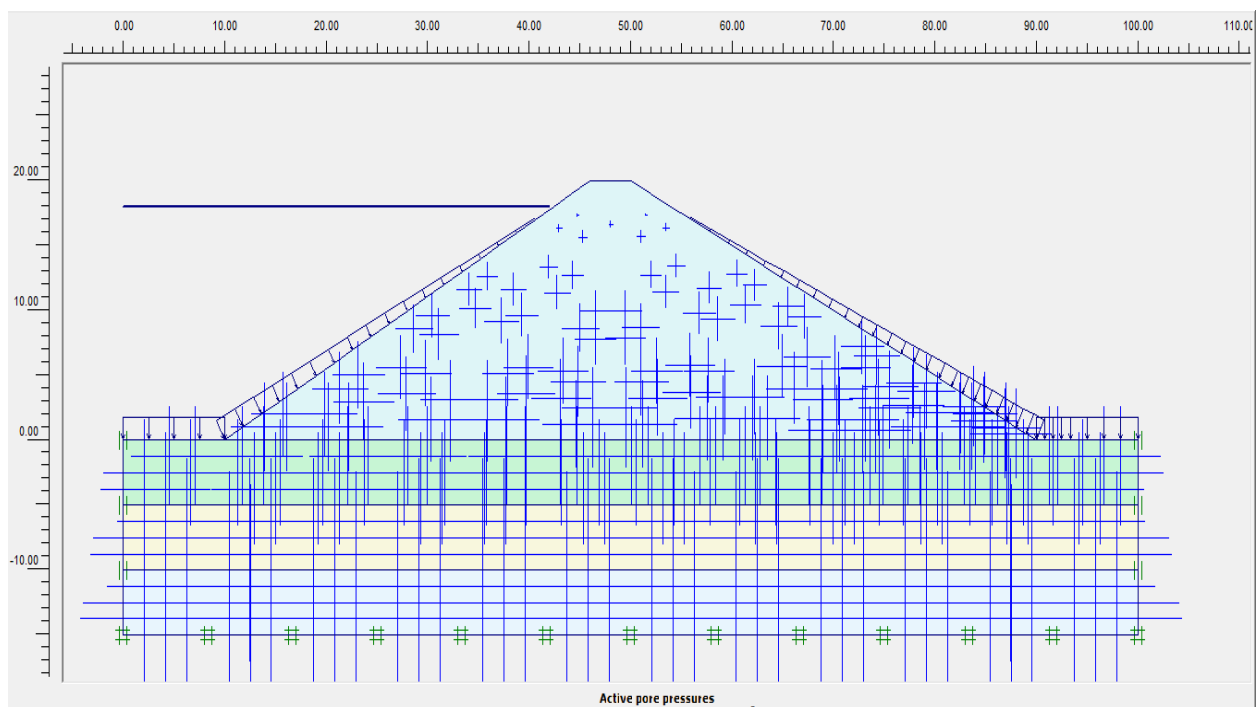


Figure 4. 11 Water table (porewater pressure distribution)

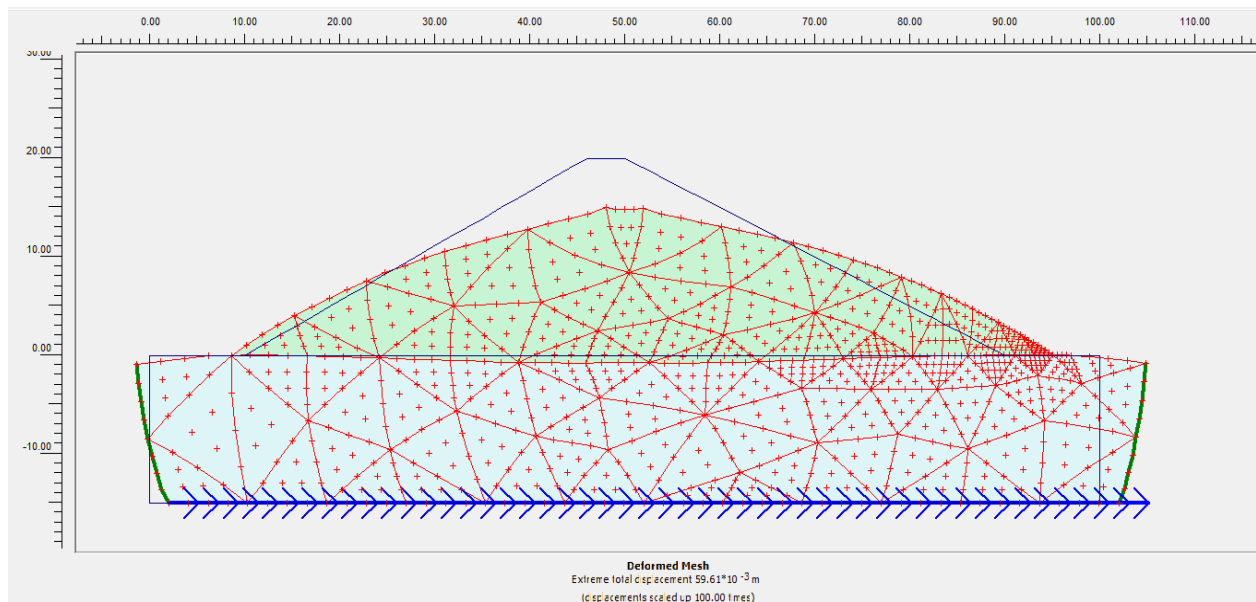


Figure 4. 12 Deformed mesh (maximum total displacement 45.89 mm)

#### 4.2.4. Excess pore water pressure

The excess porewater pressure generated due to the dynamic loading indicated that, excess porewater pressure in the silty sand foundation is greater than the relatively stiffer silty clay foundation. For the layered foundation soil, the excess porewater pressure is greater from both the aforementioned foundation soils.

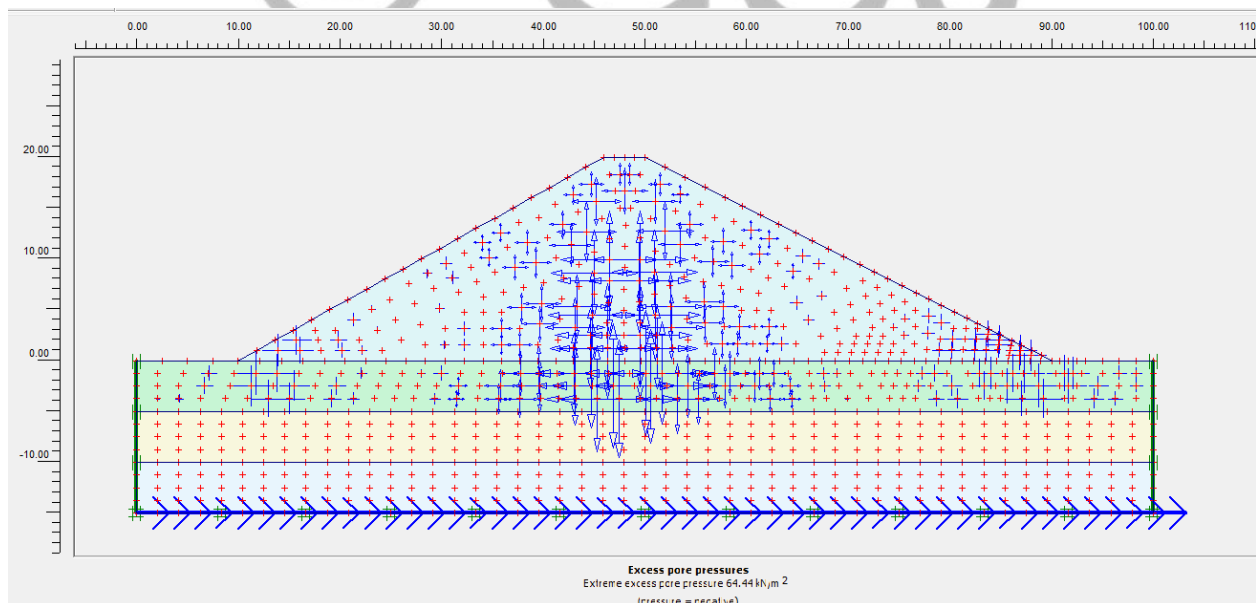


Figure 4. 13 Layered foundation soil Excess pp (max=64.44kpa)



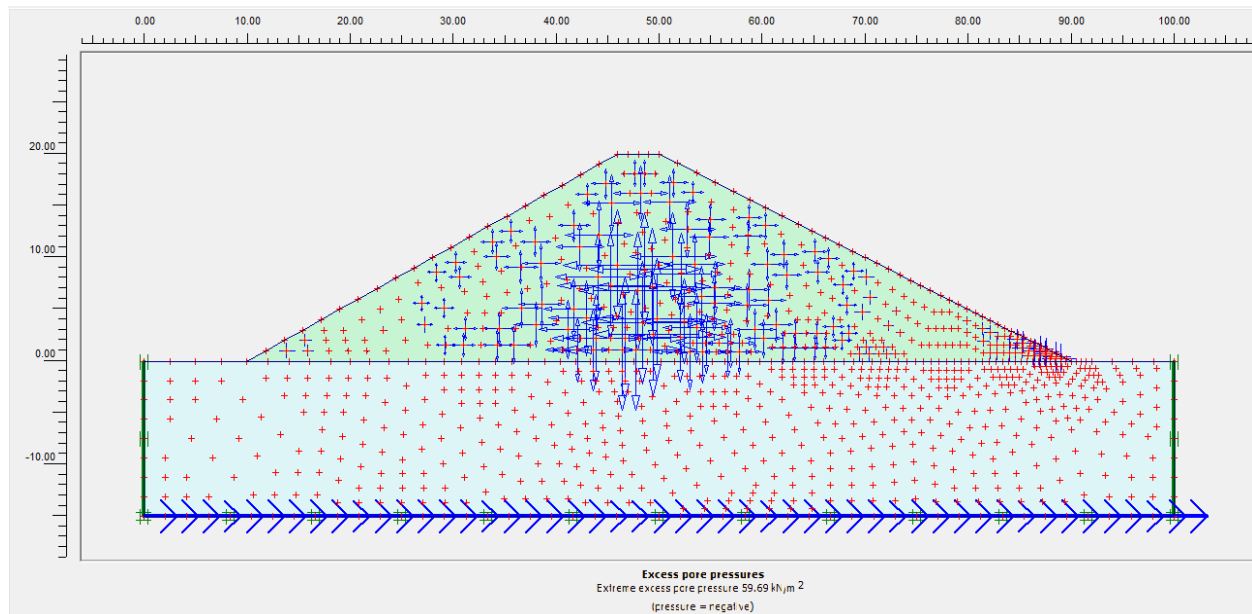


Figure 4. 14 Silty sand foundation soil Excess pp (Maximum 59.69Kpa)

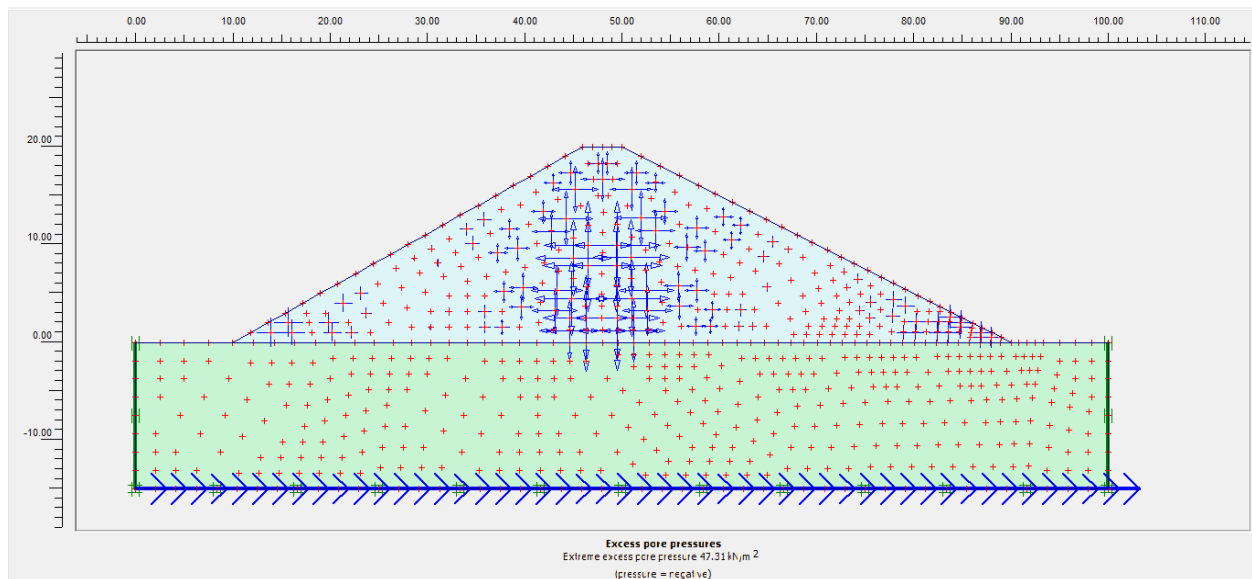


Figure 4. 15 Silty clay foundation soil Excess porewater pressure (maximum 47.31kpa)

The displacement time graph (wave propagation) at the base of the embankment over the three foundation condition indicate that; for silty sand foundation the wave propagation is greater than the silty clay and layered foundation soil conditions. The graph below shows that, the upper line is layer foundation soil. The bottom is silty sand foundation and the middle color for silty clay foundation soil. This may be due to the high damping effect of stiffer soils when exposed to dynamic loads.

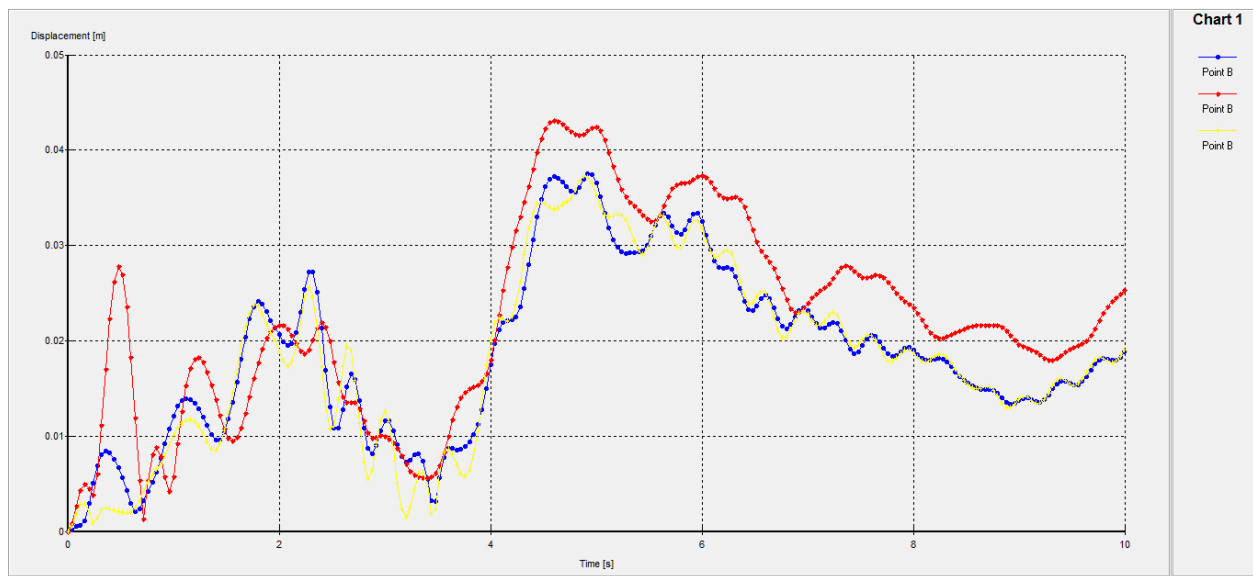


Figure 4. 16 displacement time graph (wave propagation)

### 4.3. Numerical example using the FLAC<sup>3D</sup>

#### 4.3.1. Soil property

A dam of 20 meters height is analyzed using the FLAC<sup>3D</sup> software. The material properties for the foundation and embankment dam are as given in table 3.1 to table 3.4.

#### 4.3.2. Cyclic load characteristics

To represent earthquake shaking, the dam and foundation were loaded with a cyclic load given by a sine function. The amplitude and frequency for the cyclic load are assigned to represent the earthquake shaking. The characteristics of the cyclic load are summarized in the table 3.5. The magnitudes of the amplitude and frequency are arbitrarily assigned so that the effect can easily be observed. Obviously, the characteristics of the cyclic load affect the response of the embankment and foundation. However, since this project is limited to show the effect of foundation soil property on potential dynamic instability and liquefaction problem, the cyclic load characteristics are arbitrarily assigned. The analysis procedures and result is display in the figures below.

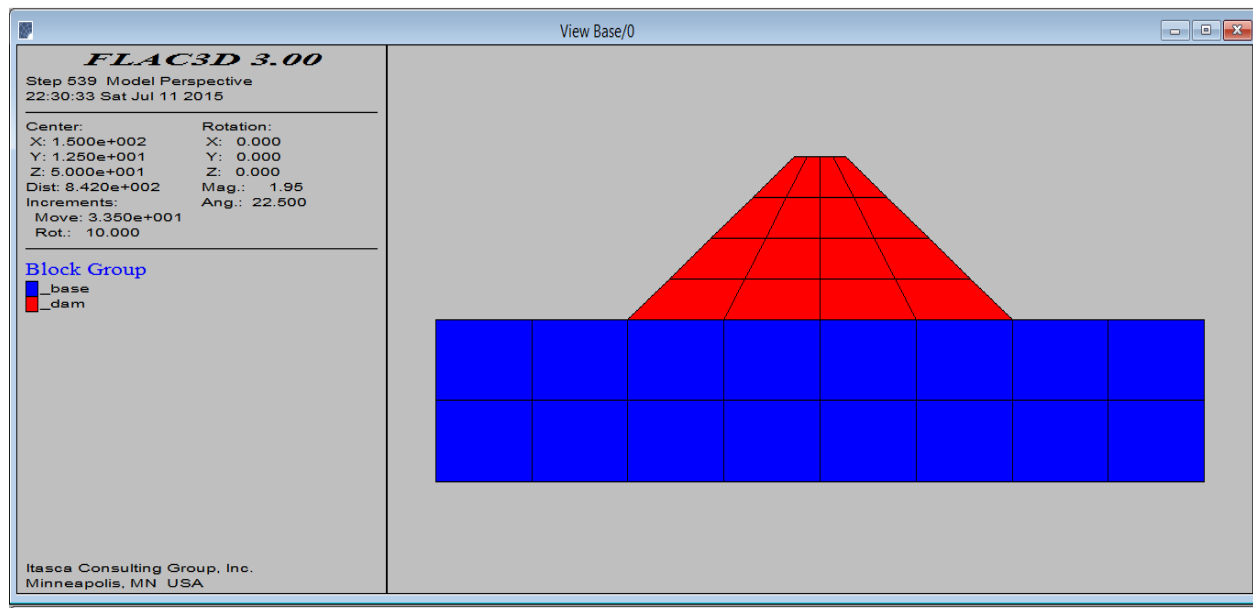


Figure 4. 17 mesh characteristics for embankment-1 and embankment-2

#### 4.3.4. Analysis result

Static analysis is done first to model the stress and strain condition of the embankments before the cyclic load is applied. Then the cyclic load is applied to represent earthquake shaking. Throughout the analysis result discussion *embankment-1* refers to the embankment resting on silty sand foundation and *embankment-2* refers to the embankment resting on silty clay soil and embankment-3 refers to embankment resting on layered foundation soil.

##### 4.3.4.1. The distribution of shaking intensity under the embankments

The distribution of maximum acceleration values were estimated under each embankment dam. The point of intersection of the embankment dam and the foundation at the center was selected to study the distribution of shaking intensity. Side view of the point selected and acceleration histories are shown below in Figures below.

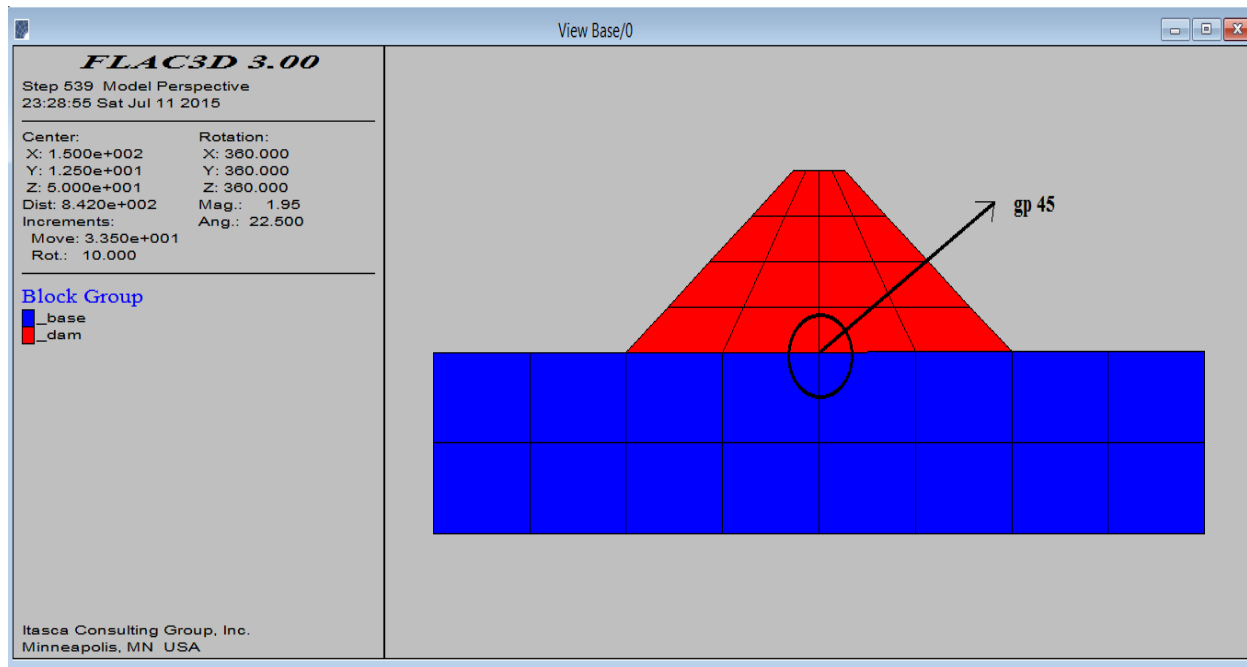


Figure 4. 18 grid point at the intersection of embankment and foundation soil (case 1 and 2)

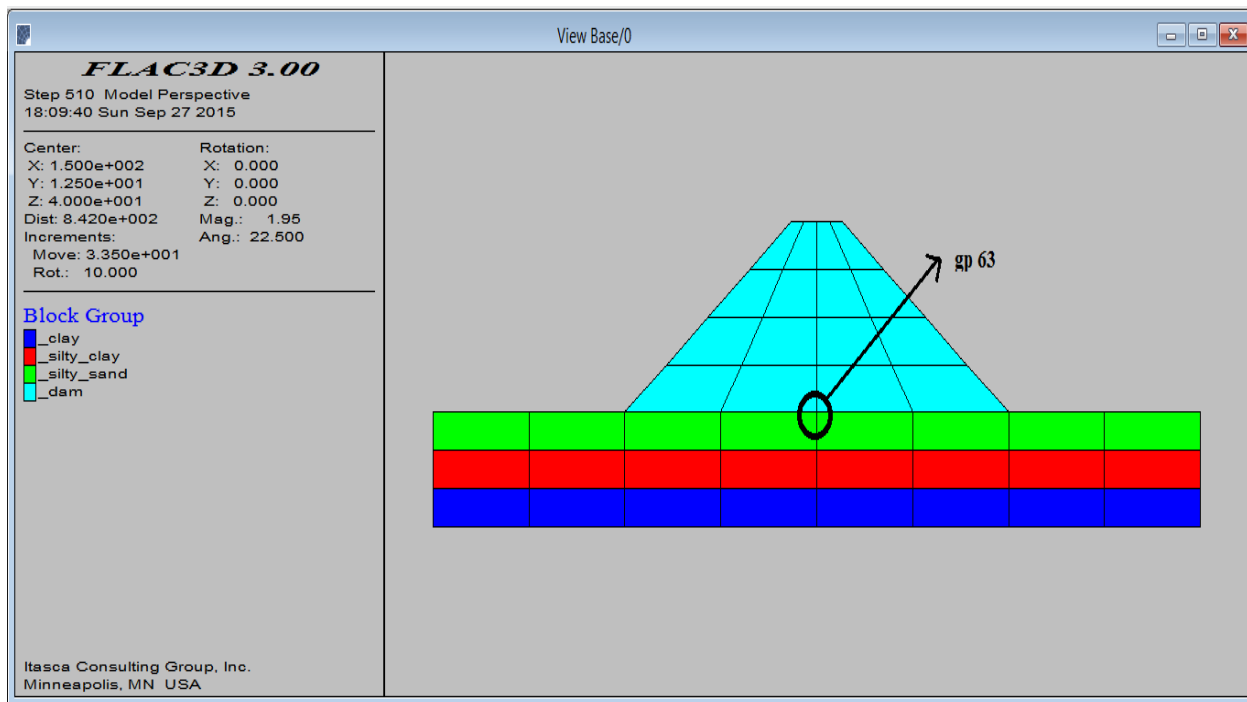


Figure 4. 19 grid point at the intersection of embankment and foundation soil (case 3)

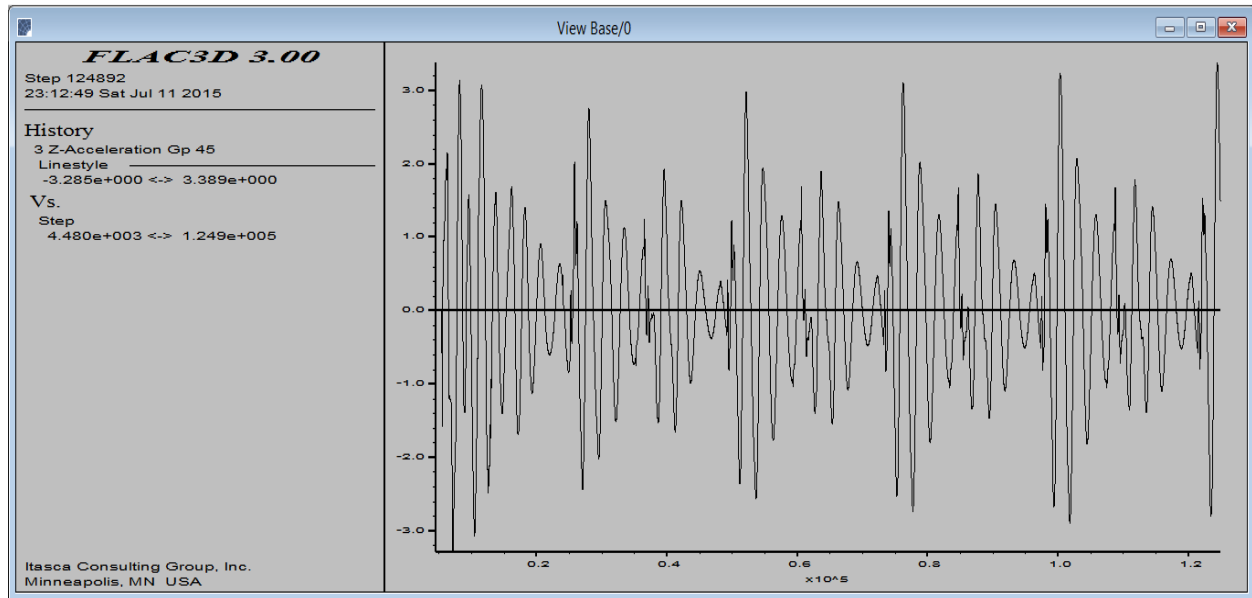


Figure 4. 20 acceleration history at grid point 45 (at the interface of the embankment-1 and foundation)

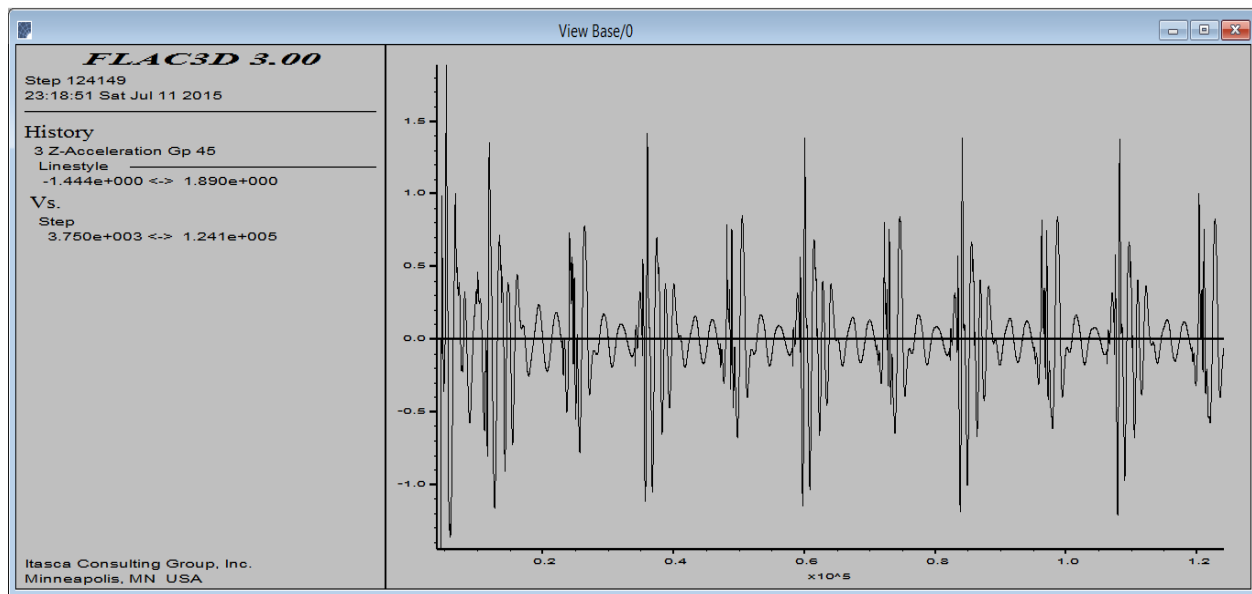


Figure 4. 21 acceleration history at grid point 45 (at the interface of the embankment-2 and foundation)

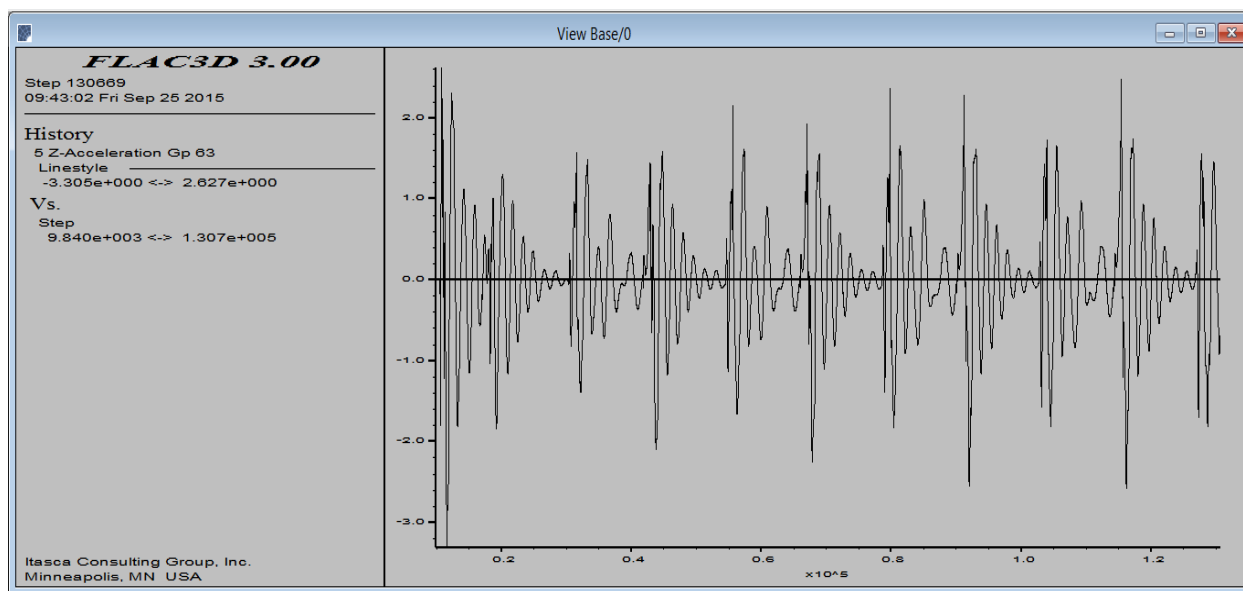


Figure 4. 22 acceleration history at grid point 45 (at the interface of the embankment-3 and foundation)

As shown on these figures, embankment-1 was shaken by a greater maximum acceleration ( $3.389 \text{ m/s}^2$ ) than embankment-2 ( $1.890 \text{ m/s}^2$ ). Embankment-3 was shaken by an acceleration value of  $3.305 \text{ m/s}^2$ . The main reason for the embankment-1 building shaken by higher acceleration values is that the silty sand soil layer deamplifies more the input cyclic load than the silty clay soil. Relatively stiffer soil layer underlay embankment-2. This has a great influence on deamplifying the input acceleration well. In some cases, soft foundations may even amplify ground shakings and induce greater problem [1].

#### 4.3.4.2. Displacement

The maximum vertical displacement of the embankment dam resting on silty sand soil is compared to maximum vertical displacement of the embankment dam resting on silty clay soil where the 10-meter silty sand soil is excavated off.

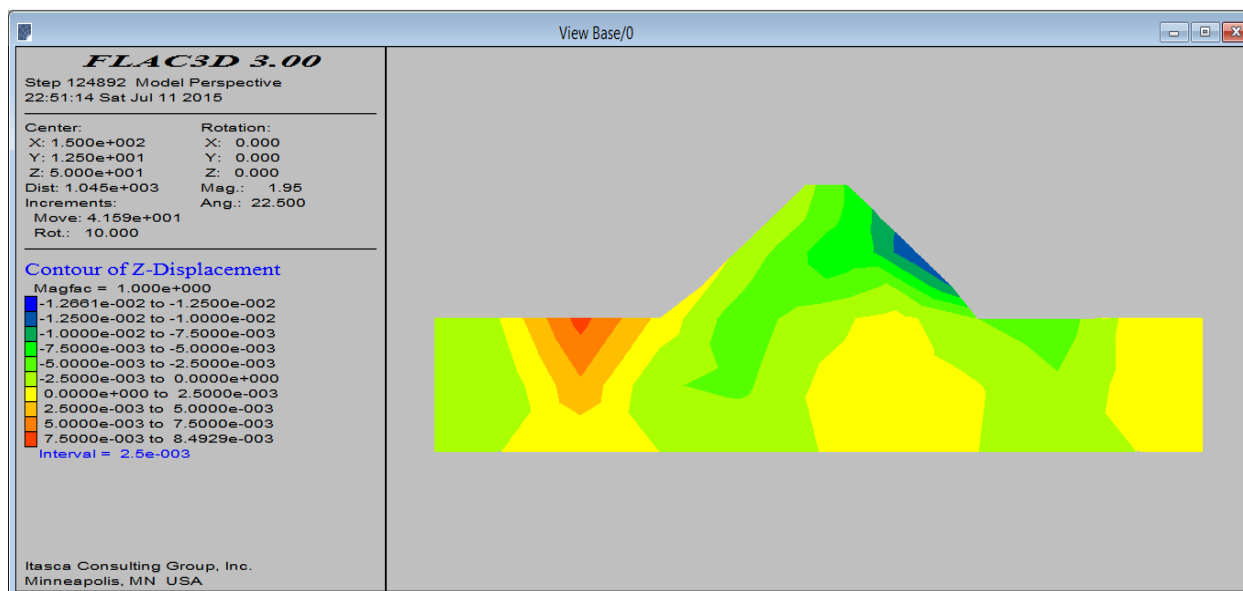


Figure 4. 23 vertical displacement of embankment-1

As can be seen from the analysis, the maximum vertical displacement (settlement) after the earthquake shaking is  $-1.2661 \times 10^{-2}$  meters. There is also upward displacement of  $8.4929 \times 10^{-3}$  meters.

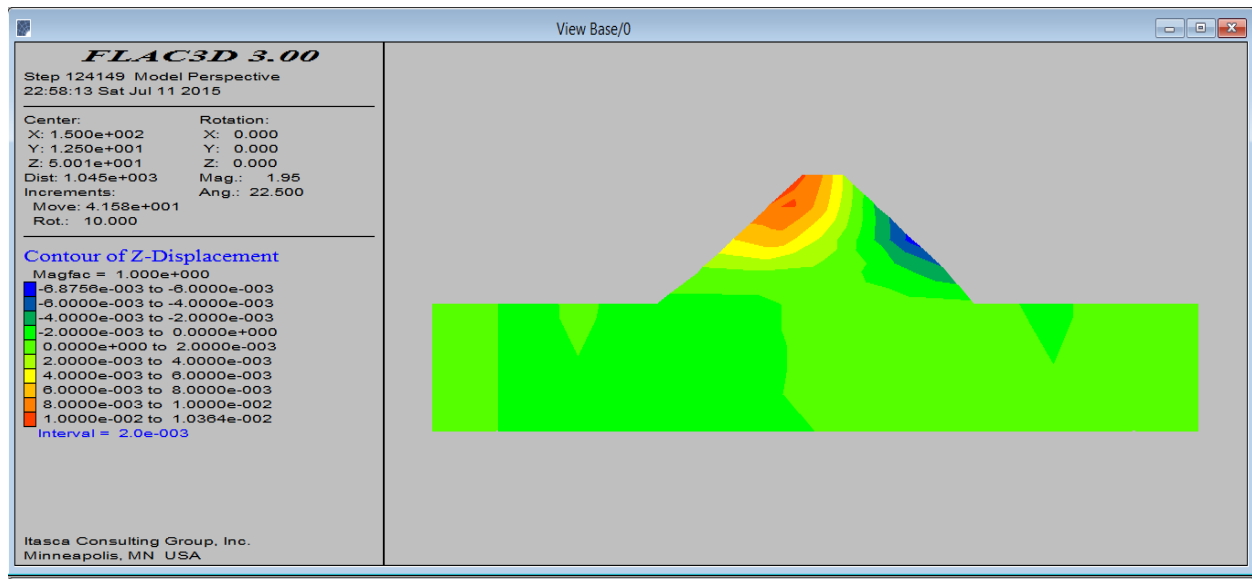


Figure 4. 24 vertical displacement of embankment -2

For embankment-2 the maximum vertical displacement (settlement) is  $-6.8756 \times 10^{-3}$  meters.

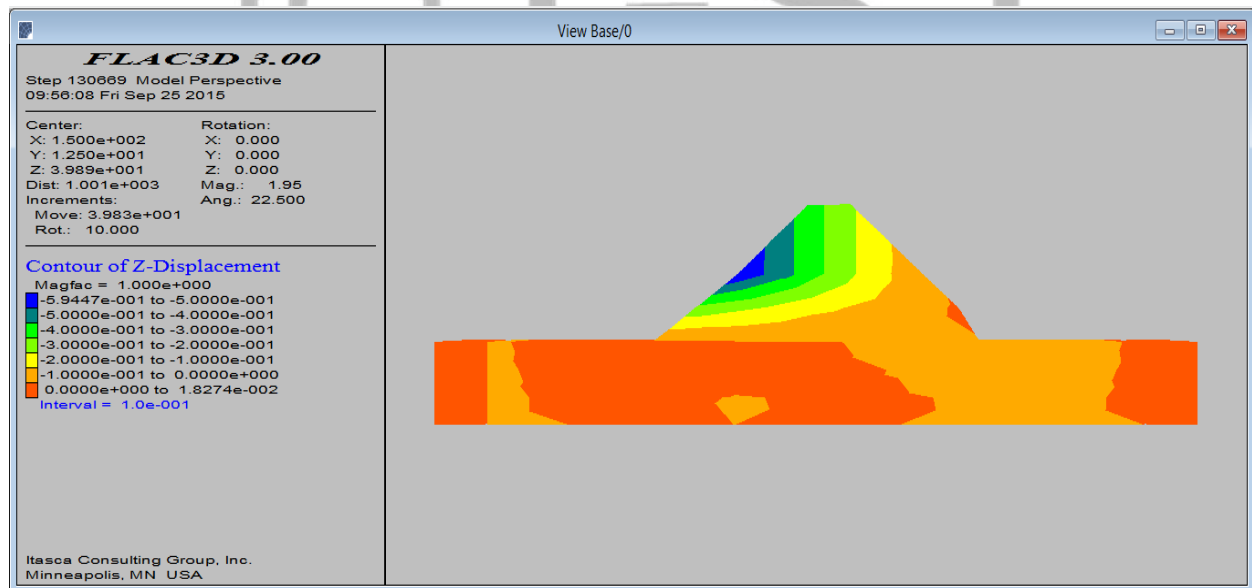


Figure 4. 25 vertical displacement of embankment -3

#### 4.3.4.3. The distribution of maximum stress, strain and pore pressure

Vertical and shear stresses as well as strain and pore pressure distributions in each embankment will be discussed next.

As shown in Figures below there is an increase as expected in the vertical stress,  $\sigma_{zz}$ , with depth for both embankments. Vertical stress is 20

KPa at the foundation level and increases to 44.7 KPa at the bottom of the foundation for embankment-1. The vertical stress is 20 KPa at the foundation level and increases to 40.8 KPa at the bottom of the foundation of embankment-2. Similarly as shown in Figures 3.25 and through 3.26 the maximum shear stresses, ( $\tau$ ), are estimated as in the range of 30-67.34 KPa at foundation level and 10 m. depth for embankment-1. For embankment-2, the maximum shear stresses, ( $\tau$ ), are estimated as in the range of 30-67.18 KPa at foundation level and 10 m. depth.

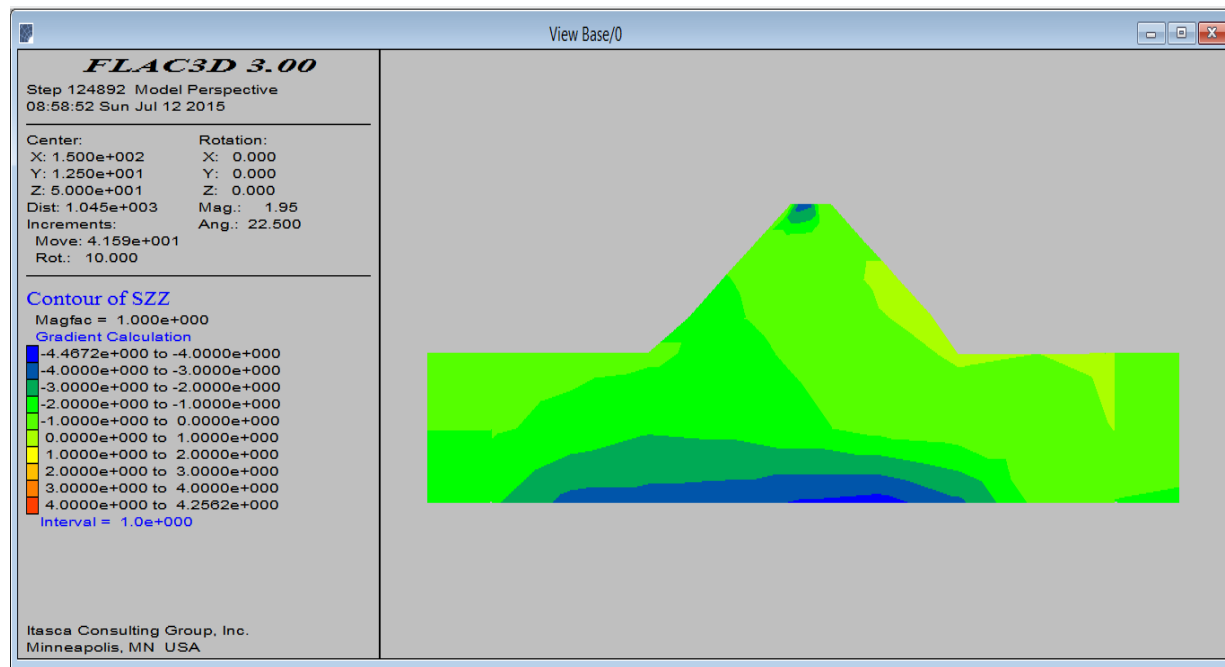


Figure 4. 26 vertical stress (  $s_{zz}$  ) of embankment -1

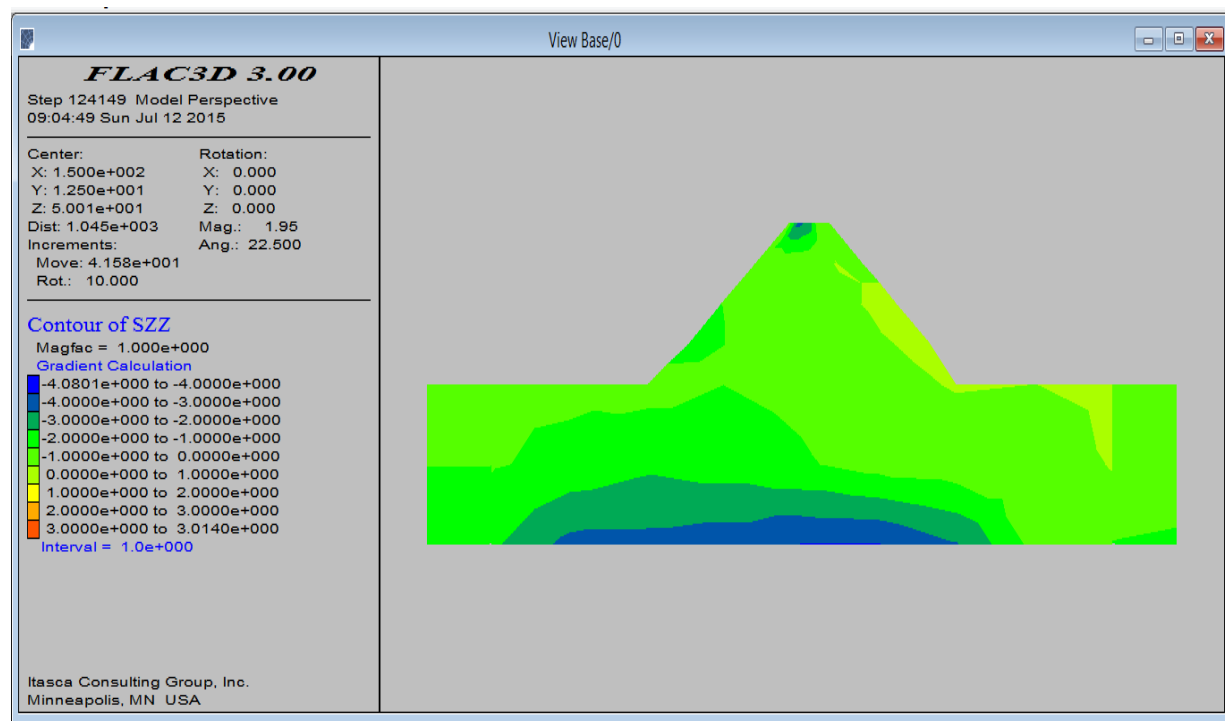




Figure 4. 27 vertical stress (  $\sigma_{zz}$  ) of embankment -2

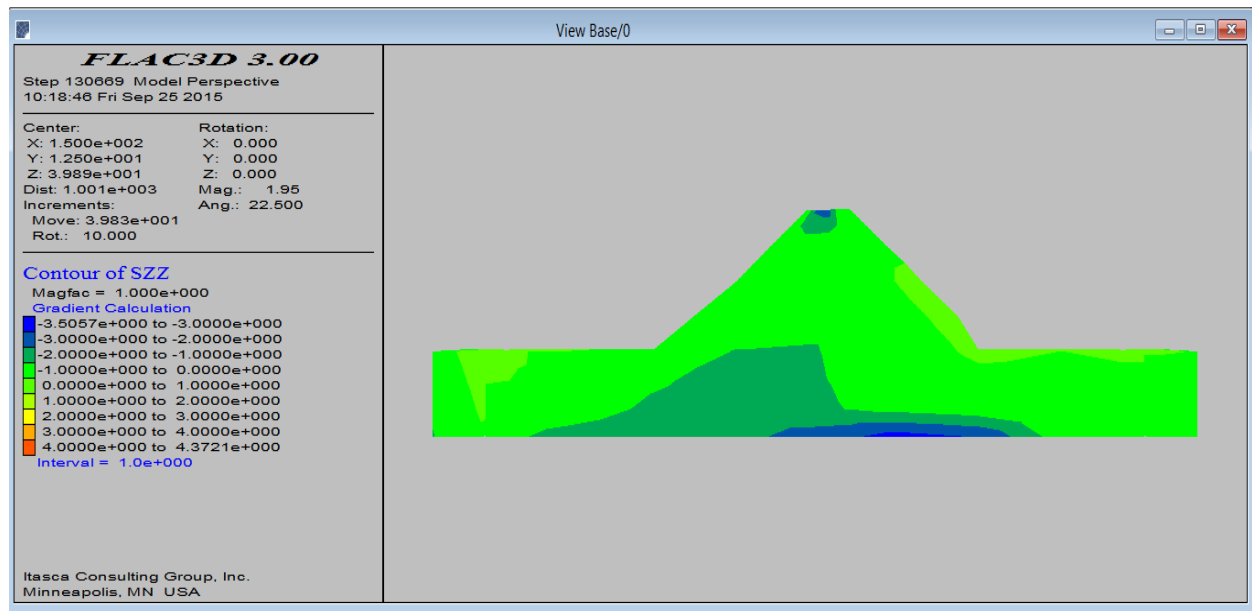


Figure 4. 28 vertical stress (  $\sigma_{zz}$  ) of embankment -3

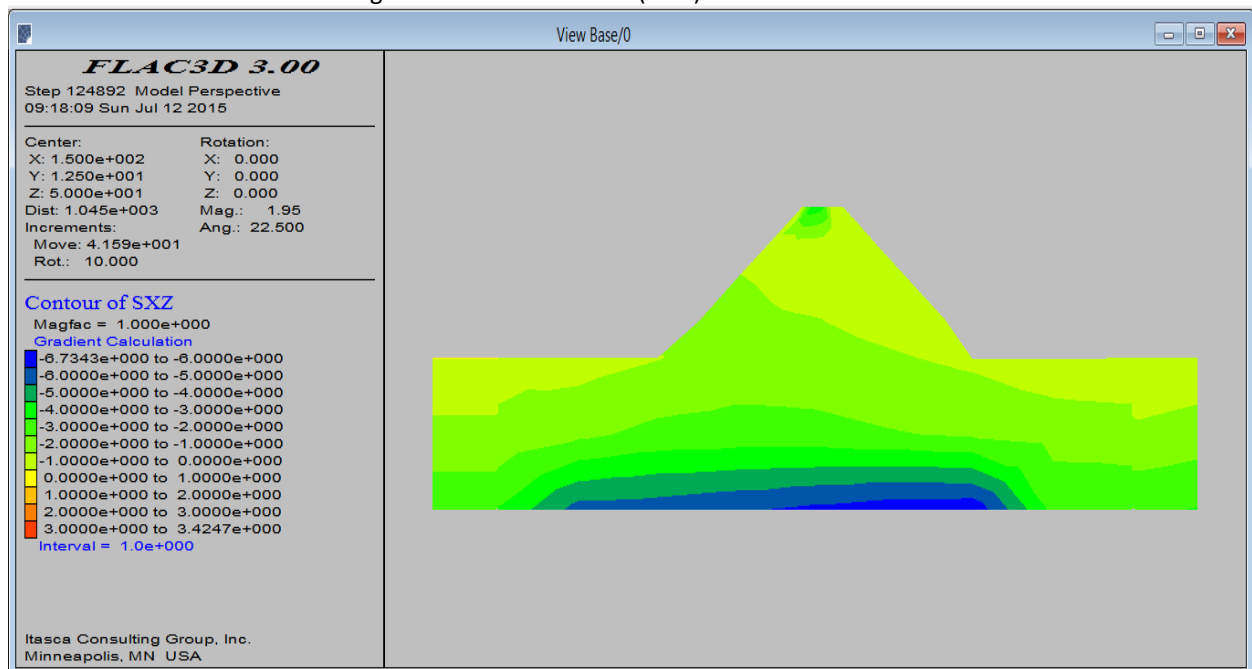


Figure 4. 29 shear stress distribution (  $\tau_{xz}$  ) of embankment -1

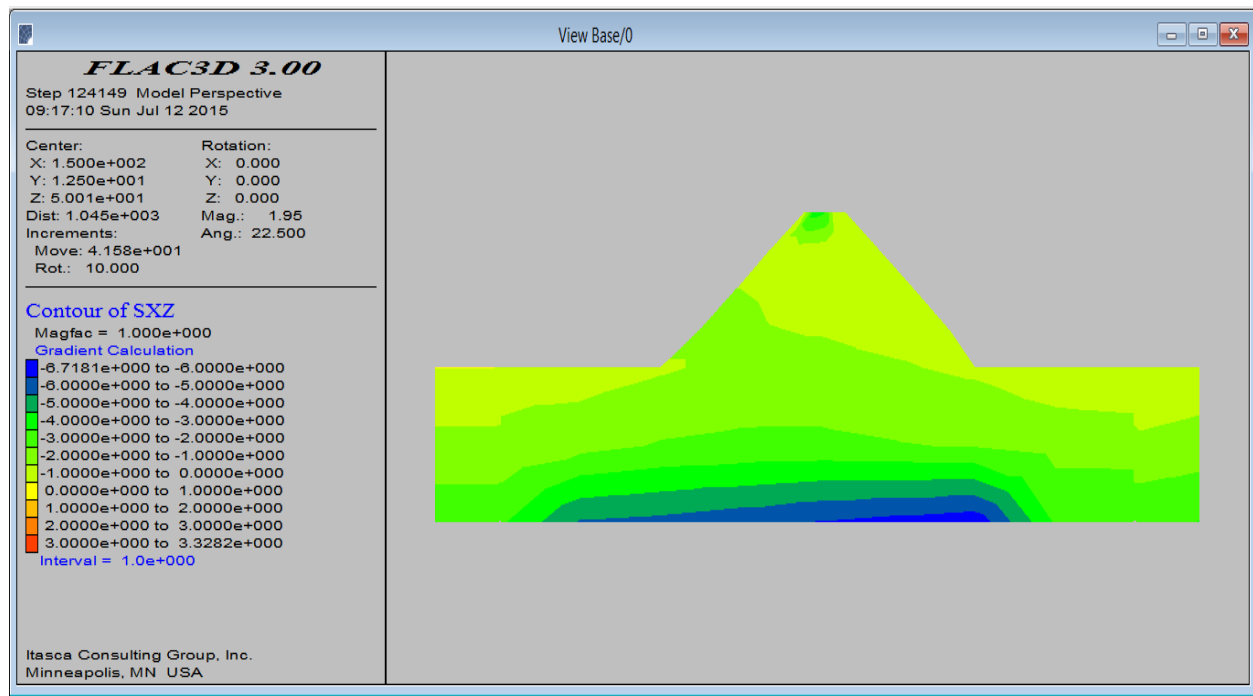


Figure 4. 30 shear stress distribution ( $\tau_{xz}$ ) of embankment -2

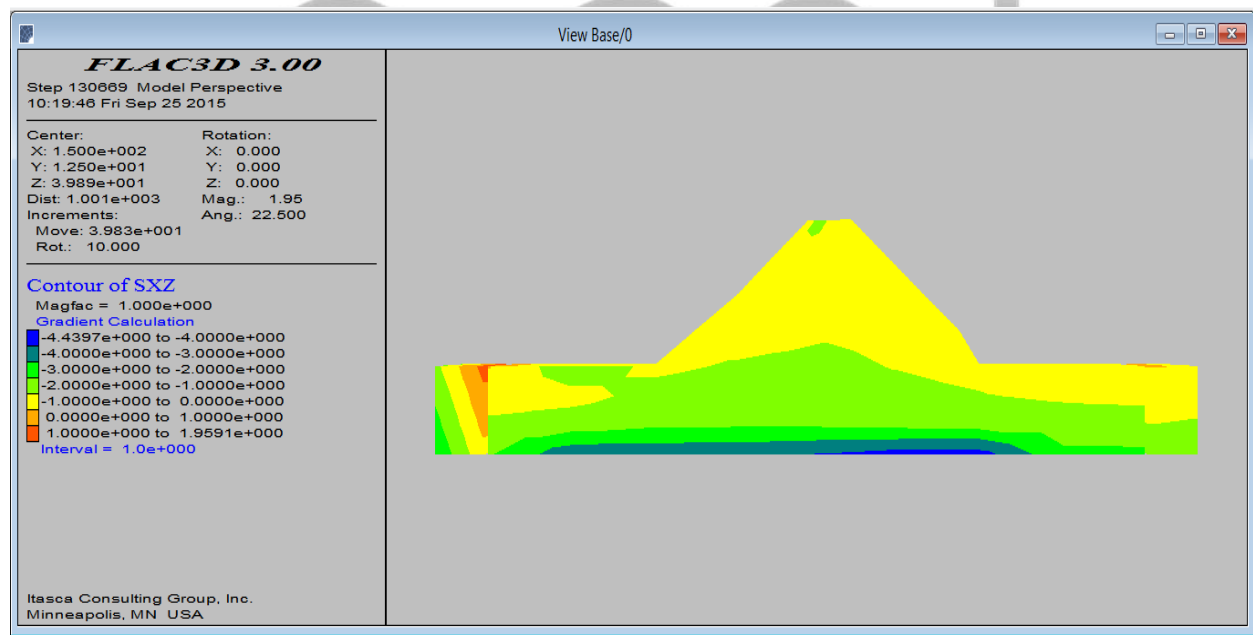


Figure 4. 31 shear stress distribution ( $\tau_{xz}$ ) of embankment -3

The analysis of shear strain histories presented in Figures below show that there is plastic yielding at various depths that increased horizontal displacements. As a similar observation it can be stated that shear strains are higher for the embankment-1 ( $\gamma=9\%$ ) to embankment-2 ( $\gamma\sim 4\%$ ). The shear strain values for the embankment-2, which lies over a relatively stiffer soil, are smaller than the embankment-1.

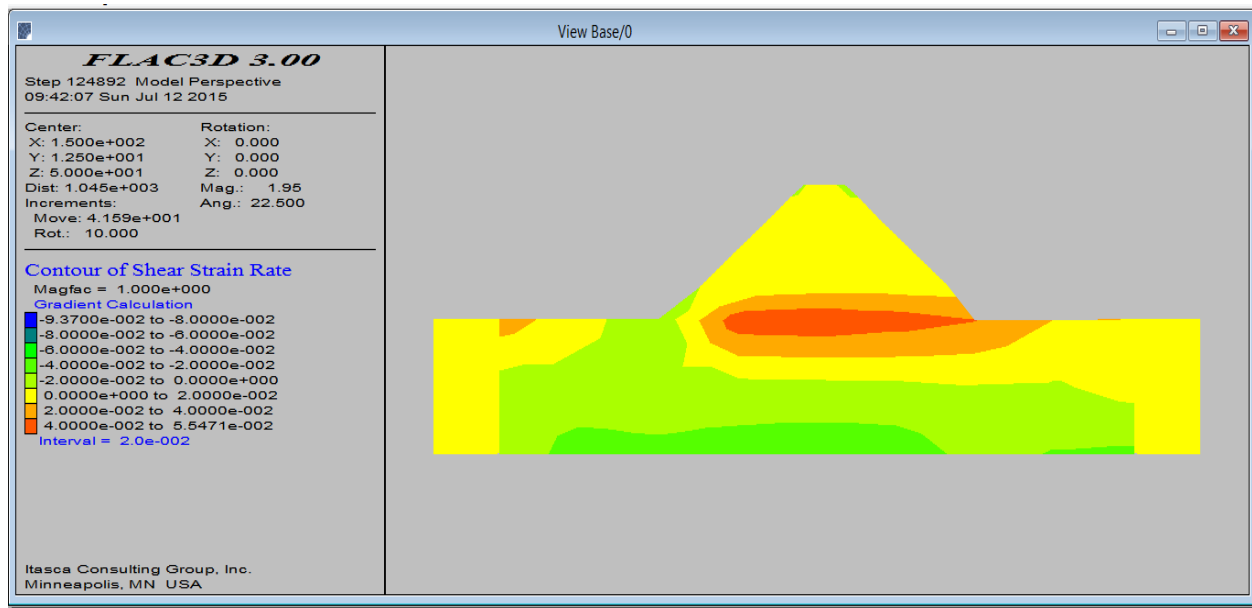


Figure 4. 32 shear strain rate of embankment -1

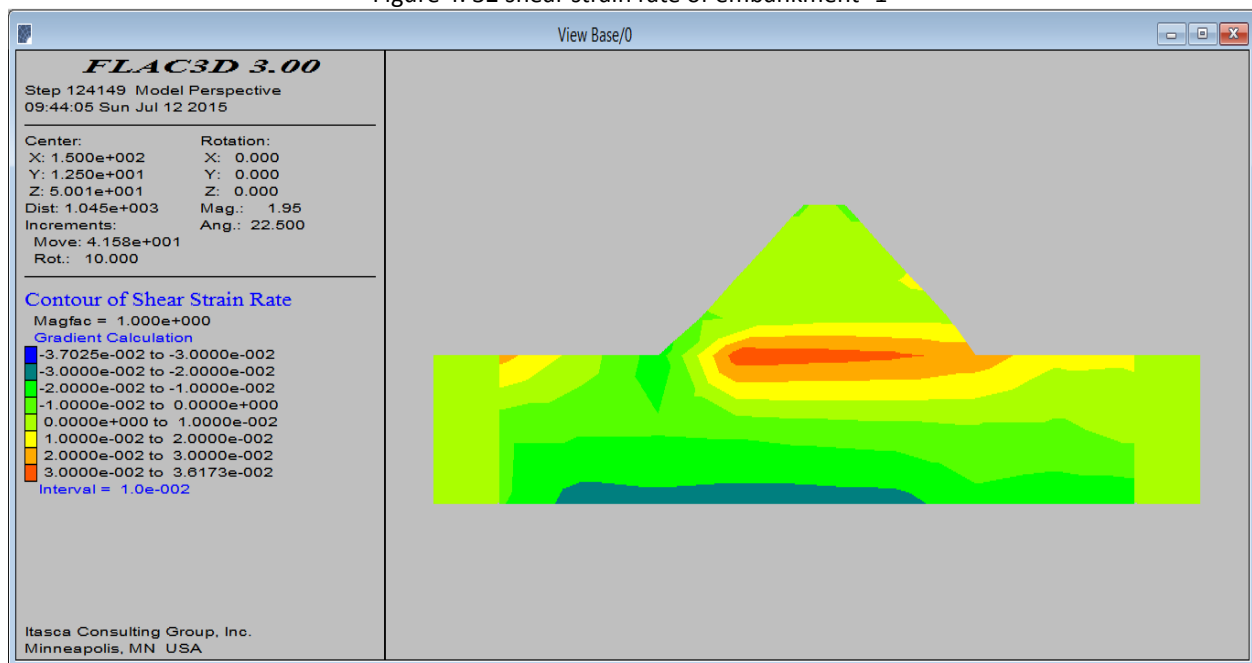


Figure 4. 33 shear strain rate of embankment -2

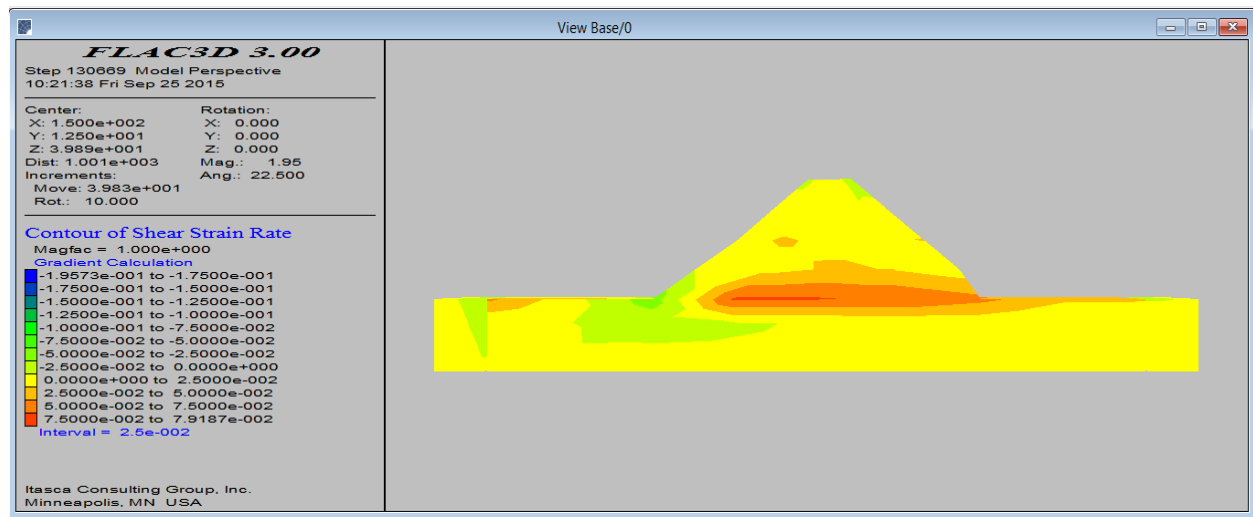


Figure 4. 34 shear strain rate of embankment -3

As shown in Figures 3.29 through 3.30 there is a gradual increase in pore pressure with depth for both embankments. The maximum pore pressure values are higher under embankment-1 than embankment-2. Higher pore pressure values are believed to be due to soil structure interaction. The values of pore pressure start with 2 KPa at about 2m depth and ends with 14.04 KPa at 10 m. depth for embankment -1. For embankment-2, the values of pore pressure start with 1 KPa at about 2m depth and ends with 11.4 KPa at 10 m.

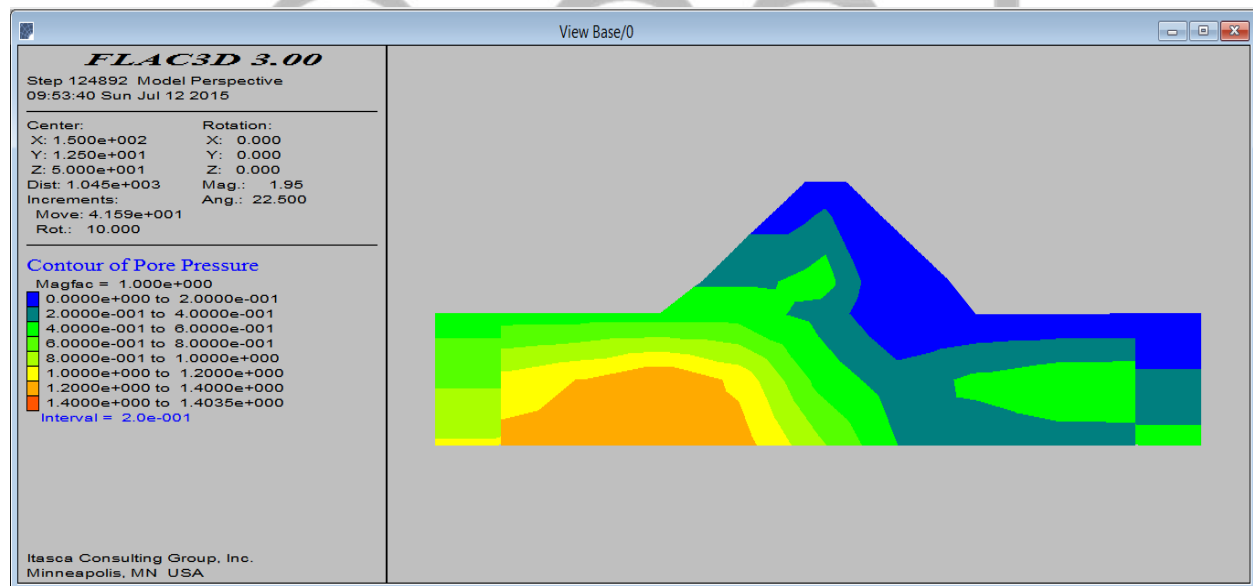


Figure 4. 35 porewater pressure of embankment -1

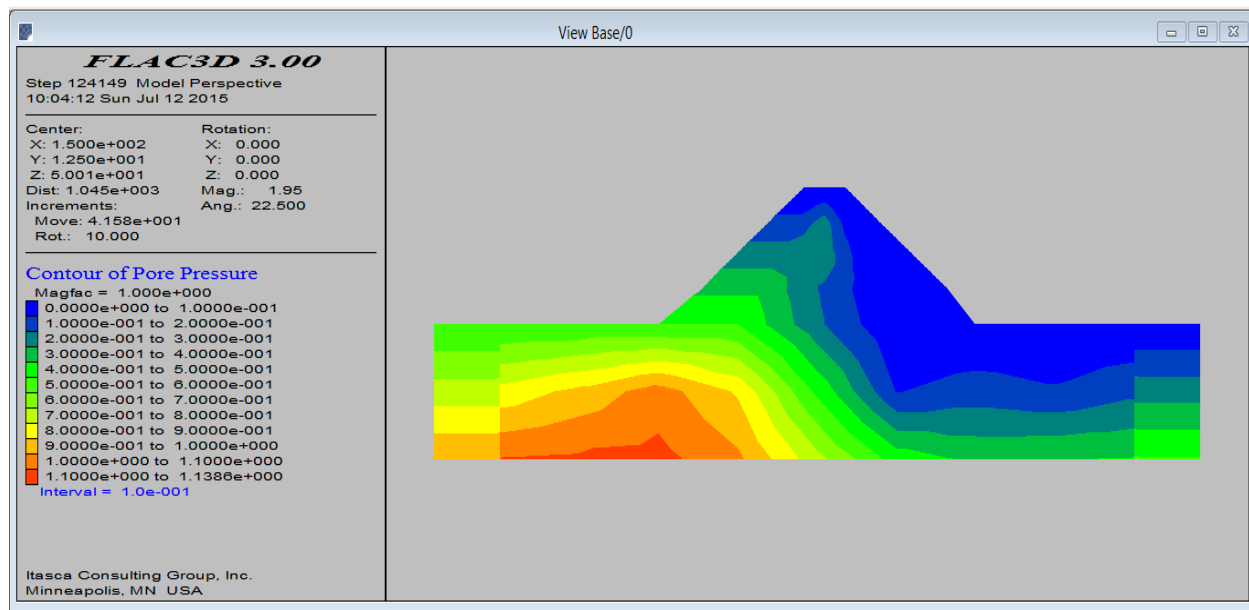


Figure 4. 36 porewater pressure of embankment -2

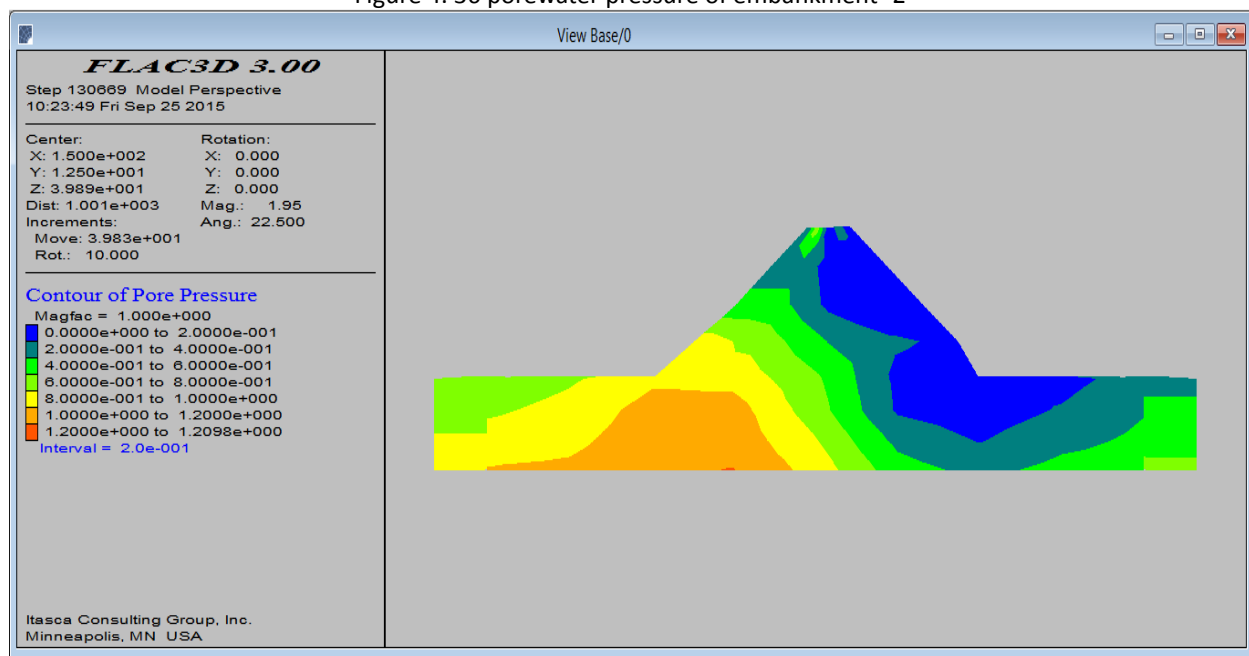


Figure 4. 37 porewater pressure of embankment -3

These high pore pressures indicate a potential liquefaction problem.

#### 4.3.4. Liquefaction assessment of the dam and foundation

From the above stress analysis result, it is observed that the porewater pressure increases with depth and attains a maximum value at 10 meters depth for both foundation soil types. This indicates that there is a potential liquefaction problem at the foundations, which will be analyzed next.

Pointed out that the foundation soil is exposed to liquefaction, the embankment and foundation soil is analyzed using the Finn model when

exposed to cyclic loading.

### ***Liquefaction Triggering Assessment***

“Simplified Procedure” as suggested by Seed and Idriss (1971) can be implemented for the purpose of estimating normalized shear stresses (CSR) developed within soil profiles during shaking. The Cyclic Stress Ratio, CSR is a measure of the cyclic load applied to the soil by the earthquake. CSR as defined by Seed and Idriss (1971) was estimated as given in Eqn (3.1) [7].

$$CSR_{\alpha} = \frac{0.65\tau_{max}}{\sigma_{v'}} \dots\dots\dots 3.1$$

Where  $\tau_{max}$  is the maximum shear stress developed during shaking and  $\sigma_{v'}$  is the vertical effective stress.

The Cycle Resistance Ratio, CRR, which is the capacity of the soil to resist liquefaction, is estimated from Standard Penetration Tests (SPT), Cone Penetration Tests (CPT) or, less frequently, the shear wave velocity. If the CSR is greater than the CRR, liquefaction is likely to occur. For most purposes a simple comparison of CSR with CRR with engineering judgment will be sufficient [1].

Vertical stresses, shear stresses, porewater pressure and effective stress and values were estimated as part of the dynamic analyses and were presented in Figures above.

The CSR value for embankment-1 is around 1.427 at the bottom of the foundation. On the other hand, the values changes to 1.465 for embankment-2. The higher CSR values of embankment-2 indicate that embankment-1 is more prone to liquefaction.

The related figures show that the Liquefaction potential is higher under embankment-1 than under embankment-2 which may be due to the soft soil under embankment-2. Below, the figures show that the dynamic porewater pressures at different zones are greater in embankment-1 than embankment-2. This is may be due to the cyclic load is deamplified more in embankment two and thus the effect is reduced.

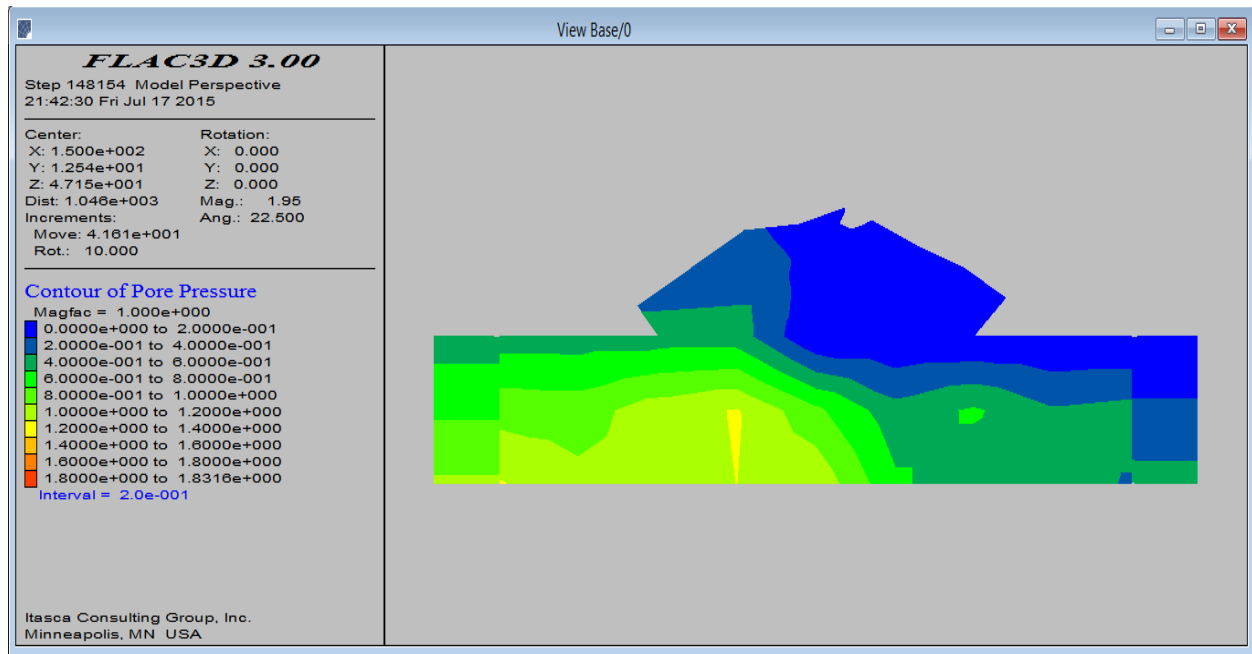


Figure 4. 38 dynamic porewater pressure history for embankment-1

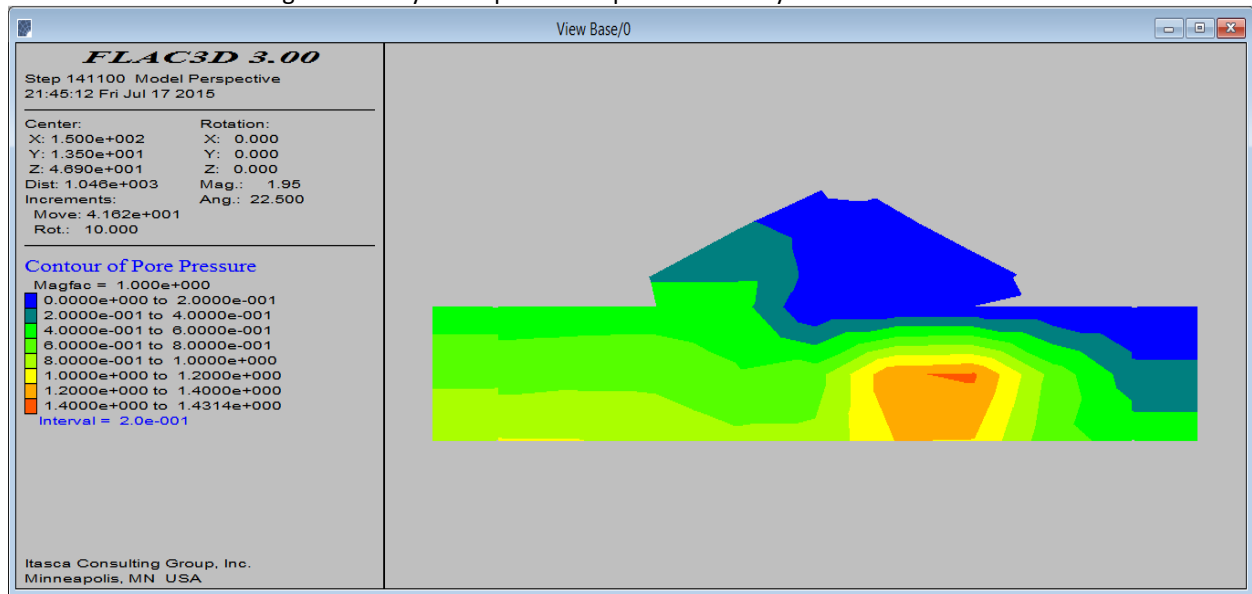


Figure 4. 39 dynamic Porewater pressure for embankment-2

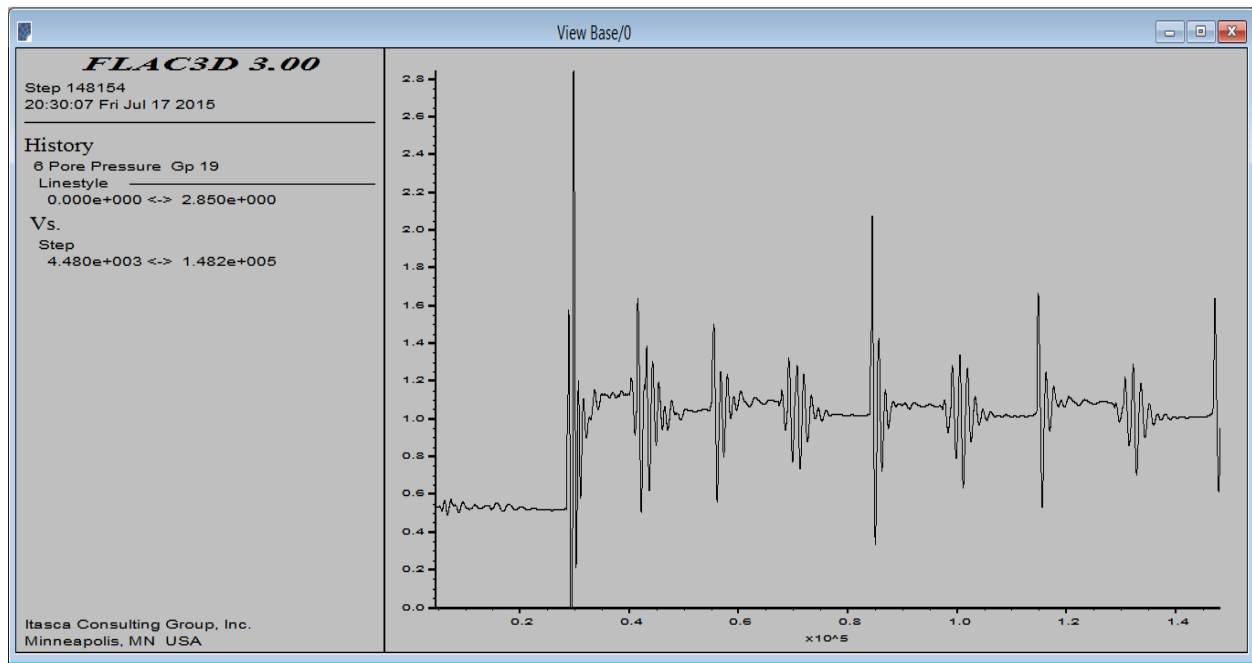


Figure 4. 40 dynamic porewater pressure history for embankment-1at the foundation

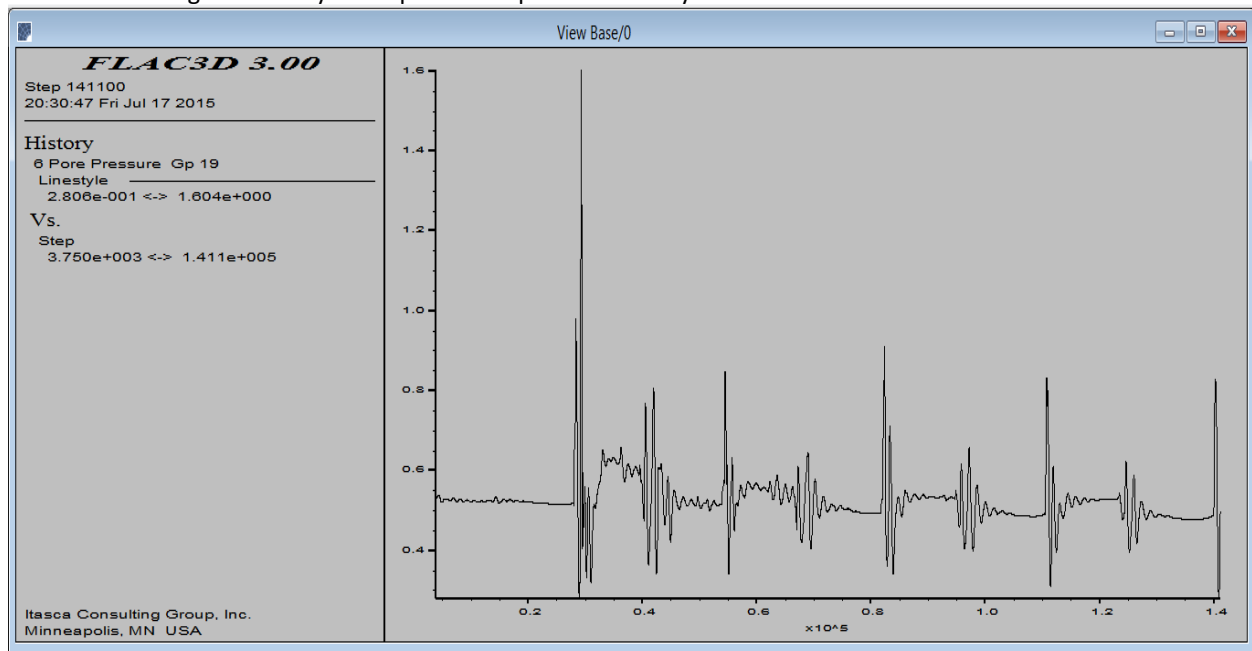


Figure 4. 41 dynamic Porewater pressure history for embankment-2 at the foundation



## 5. RESULTS AND DISCUSSION

### 5.1. Introduction

In this chapter, the results of numerical illustration of all the cases done using both the FLAC<sup>3D</sup> and PLAXIS geotechnical softwares are summarized and discussed. The results of the analysis using the FLAC<sup>3D</sup> and PLAXIS softwares are compared to each other respectively.

Dynamic response analysis of soil was done to see the effects of foundation soils on the identical embankments. 2-D cross-sections of the site of estimated soil layers were constructed based on reasonably assumed data [3]. After determining the soil properties of these layers and the embankment, 2-D mesh models of the site were constructed. First static analyses were performed. The aim of performing static analysis was to obtain static force equilibrium, which would be used in the dynamic analysis.

Secondly input ground motion was constructed. A cyclic load given by a sine function was used to represent dynamic loading (earthquake) in FLAC<sup>3D</sup> and an available earthquake record was used in PLAXIS.

Finally the dynamic analysis was performed. First, the embankment and foundation soils were analyzed together using isotropic fluid flow and Mohr-Coulomb plasticity models to see effect of cyclic loads on overall performance of the two embankments. On the next step, the finn model was used to observe dynamic porewater distribution of the embankment and foundation using the FLAC<sup>3D</sup>. Finn model parameters for the dynamic analysis were reasonably assumed. Viscous boundary conditions were applied and the 2D dynamic nonlinear analysis of the site was done by using the computer program FLAC<sup>3D</sup>.

### 5.2. Results of numerical illustration using the PLAXIS and FLAC<sup>3D</sup> geotechnical software

The result of the numerical illustration using the PLAXIS is summarized in the table below for the three cases. The analysis result is presented in the form of extreme total displacement, strain, excess porewater pressure and effective vertical stress.

*Table 5. 1 Summery of analysis result using the PLAXIS*

Property	Foundation Soil Condition		
	Silty sand	Silty clay	Layered
extreme total displacement (mm)	59.61	47.32	45.89
Extreme vertical strain (%)	0.2879	0.28497	0.23454
excess pp (kPa)	59.69	47.09	64.44
vertical effective stress (kPa)	326.77	352.45	370.35

From the analysis result it can be seen that;

- The total deformation due to earthquake loading is higher for the embankment dam founded on silty sand soil. On the relatively stiffer silty clay and layered foundation soils, the embankment deformation is lesser.

- The extreme vertical strain for embankment founded on silty sand foundation soil is also higher than that of silty clay and layered foundation soils.
- The porewater pressure developed on the embankment founded on layered soil is greater than the silty sand and silty clay foundation soils. Nevertheless, the vertical effective stress is greater than both. The porewater pressure developed on the silty sand foundation is higher than that of silty clay foundation and it has the smallest vertical effective stress.

In conclusion, it can be seen that embankments founded on soft foundation soils are highly at risk to dynamic load induced instability.

The result of the FLAC<sup>3D</sup> analysis is also given in the table below. In the FLAC3D analysis, the earthquake-induced liquefaction is also assessed for the two foundation cases. The analysis for the third case took longer time and result is not estimated.

*Table 5. 2 Summery of Analysis result using the FLAC3D*

Property	Foundation soil condition		
	Silty sand	Silty clay	Layered
Maximum acceleration time history (m/s <sup>2</sup> )	3.389	1.89	3.305
Maximum vertical displacement (m)	0.01266	0.0068756	0.59447
Maximum vertical stress (kPa)	447	408	350.57
Maximum shear stress (kPa)	673.4	671.8	443.97
Maximum shear strain (%)	9.37	3.7	19.57
Maximum porewater pressure (kPa)	140.4	114	120.9
CSR	1.427	1.465	
Maximum dynamic porewater pressure (kPa)	18.32	14.31	

As a result of the project, the following observations were made which could potentially explain different levels of dynamic instability at two identical embankments resting on different soil layers.

- Embankment-1 was estimated to be shaken by a maximum acceleration of 0.34g whereas embankment-2 was estimated to be shaken by a maximum accelerations of 0.29g at same location respectively when exposed to same cyclic load. These different intensities of shaking could be potentially explained by the variation of the stiffness of the foundation soil. relatively stiffer soil is found under embankment-2. The shaking intensity for embankment-3 is slightly less than embankment-1
- The maximum strains (9.37%) for embankment-1 during the earthquake were found to be higher than that of embankment-2 (3.7 %) It is believed that high shear strain values may negatively affect the embankment performance during earthquake.
- A relative vertical displacement of approximately 12 mm, and 6 mm. are estimated for the embankment-1 and embankment-2 respectively on dynamic analysis. 59 mm vertical displacement is estimated for embankment-3. The maximum displacement values embankment-2 are much smaller than that of embankment-1 and embankment-3 which is highly settled during the earth-

quake. Even though calculated vertical displacements of the three embankments deviate very much, they are believed to be a good indication of embankment performance.

- Although the pore pressure values are large for both embankments, it can be concluded that embankment-1 is the one that is most affected due to the soil stiffness loss (liquefaction).
- The element sizes of the mesh are large and since the exact degree of incompressibility cannot be estimated, some accuracy losses occur in the computer models.

The vertical displacement and vertical effective stress for the three cases using both the FLAC3D and PLAXIS geotechnical softwares are summarized in the tables below for comparison.

*Table 5. 3 Maximum vertical displacement*

Maximum vertical displacement (mm)			
	case one	case two	case three
FLAC <sup>3D</sup>	12	6	59
PLAXIS	51.7	41.76	39.95

*Table 5. 4 Maximum vertical effective stress*

Vertical effective stress (kPa)			
	case one	case two	case three
FLAC <sup>3D</sup>	447	408	350.7
PLAXIS	326.77	352.45	370.35

The variation in the results of the two geotechnical softwares is due to the difference in the dynamic loading characteristics and depth of foundation soil modeled.

## Conclusion

The results of this study revealed that there could be major changes in foundation soil profiles, which in turn may affect the performance of embankments founded on these soils when dynamic stability is considered.

- The numerical illustrations results revealed that there is a major difference in deformation, stress and porewater pressure distribution when embankments resting on different foundation soils are exposed to equal magnitude of dynamic loading.
- The deformation, stress and porewater pressure magnitudes are generally larger for an embankment resting on relatively loose foundation when compared to embankment resting on stiffer foundation.
- The results support the importance of soil site investigations for dynamic loading before the design of overlying structures.
- In cases of resting an embankment on loose soils like alluvium deposits, dynamic load induced instability needs to be considered and checked thoroughly.
- There is obviously some loss of accuracy on the numerical illustrations due mesh size and characteristics.
- In addition, the characteristics of the dynamic loading used in the illustrations done using PLAXIS are not an actual dynamic load.

## Recommendations

Nowadays large dams are being planned and constructed in different parts of Africa for community water supply and irrigation developments. In Ethiopia, in the rift valley region, a number of dams are proposed and being constructed. The Tendaho dam is one of the dams in the region. This region is a known seismic area. Seismicity should always be considered in designing dams in seismic prone areas. A systematic understanding of the effect of seismic load on the performance of dams helps in safe design of dams. Generally;

- Foundation soil dynamic property investigation and analysis is mandatory in embankment dams located in earthquake prone areas.
- Detailed case study on performance of embankment dams located in earthquake areas should to be done for a more accurate reliable result.
- 3D modeling and use of latest version of the geotechnical softwares used in this study could give better results.

## Acknowledgment

The authors wish to thank Addisizemen Teklay (PhD) and Acham Abit for their valuable comments.

## References

- [1] P. Novak, A.I.B. Moffat, C. Nalluri and R. Narayanan, (2007) "Hydraulic Structures", Fourth Edition, Taylor & Francis 270 Madison Ave, New York, NY 10016, pp. 42-116
- [2] Kramer, S. L. (1996), "Geotechnical Earthquake Engineering", Prentice Hall, Upper Saddle River, New Jersey
- [3] Orhan Ünal, (2003) "3-d soil structure interaction analyses of three identical buildings in sakarya city after 17 august 1999 kocaeli earthquake", Middle East Technical University
- [4] Robin Fell, Patrick MacGregor, David Stapledon, Graeme Bell (2005) "Geotechnical engineering of dams" A.A. Balkema Publishers Leiden, The Netherlands
- [5] Braja.M.Das (1997) Advanced Soil Mechanics, 2nd edition, California state university
- [6] Kuhlmeier, R.L., Lysmer, J.(1973) " Finite Element Method Accuracy for Wave Propagation Problems." J. Soil Mech. & Foundations, Div. ASCE, 99(SM5), 421-427 (May).
- [7] Seed, H.B., Idriss, I.M.(1971) "Simplified procedure for evaluating soil liquefaction potential" Journal of the Soil Mechanics and Foundations Division ,ASCE, vol 107,No. SM9, pp.1249-1274
- [8] Finn, W.L., Byrne, M.P., Martin, G.R.(1976)"Seismic Response and Liquefaction of Sands" Journal of the Geotechnical Engineering Division ,ASCE, vol 102,No. GT8, August.
- [9] Itasca Consulting Group, (2002) "Flac3D manual", Minneapolis, USA.